

NASA Contractor Report 3748

# DC-10 Winglet Flight Evaluation Summary Report

A. B. Taylor

CONTRACT NAS1-15327  
DECEMBER 1983



25th Anniversary  
1958-1983

**NASA**

NASA Contractor Report 3748

# DC-10 Winglet Flight Evaluation Summary Report

A. B. Taylor  
*McDonnell Douglas Corporation*  
*Long Beach, California*

Prepared for  
Langley Research Center  
under Contract NAS1-15327

**NASA**  
National Aeronautics  
and Space Administration

**Scientific and Technical  
Information Branch**

1983

## FOREWORD

This document is the summary report of the DC-10 Winglet Flight Evaluation program which was conducted as one task of Contract NAS1-15327 under the NASA Energy Efficient Transport (EET) project. The evaluation program included Douglas-sponsored work.

The NASA Technical Monitor for this contract was Mr. T. G. Gainer of Langley Research Center. The on-site NASA representative was Mr. J. R. Tulinius. Acknowledgment is also given to the Director and staff of Dryden Flight Test Center for their assistance during the program.

The work was conducted by Douglas Aircraft Company at its facilities at Long Beach and Yuma, and at Edwards Air Force Base. Key program personnel were:

M. Klotzsche	Aircraft Energy Efficiency (ACEE) Program Manager
A. B. Taylor	EET Project Manager
P. T. Sumida	Task Manager (also Detail Design subtask)
W. P. Perks	Manufacturing subtask
W. B. Jones	Aircraft Preparation subtask
C. H. Fritz	Laboratory Test subtask
V. A. Clare	Flight Test subtask
D. J. Thomas	Loads Measurement Program
J. T. Callaghan	Aerodynamics
J. E. Donelson	Aerodynamics

## SUMMARY

This report summarizes the results of a flight evaluation of winglets on a DC-10 Series 10 transport aircraft. The objectives of the program were to determine the effect of winglets on aircraft performance and flying qualities (by conducting back-to-back flight tests with and without winglets), to gather flutter-related data, and to determine the effect of winglets on flight loads.

The basic winglet configuration used initially in the tests was directly related to the designs developed by Dr. R. T. Whitcomb of NASA Langley Research Center. The configuration had a large upper winglet and a small lower winglet. A truncated version of the upper winglet was also tested to evaluate the effect of reducing the span.

During the initial flight tests of the basic winglet, low-speed buffet was encountered. A number of alternative configurations were therefore developed and tested, several of which achieved acceptable low-speed buffet characteristics. The greatest low-speed drag reduction was achieved with leading edge devices on the upper and lower winglets. Lower winglets were required for maximum drag reduction in both cruise and low-speed flight regimes. The addition of outboard aileron droop to the reduced span winglet configuration enhanced the cruise benefit of winglets.

Winglets had no significant impact on stall speeds, high-speed buffet boundary, or stability and control characteristics. The flutter tests did not reveal any unforeseen behavior, as the test results agreed with the analytical predictions and ground vibration data. Data from the loads measurement program, which were produced in a concurrent Douglas task, were also in agreement with predictions.

It was estimated from the test results that the application of the reduced-span winglet and aileron droop to a production version of the current DC-10 Series 10 aircraft would yield a 3-percent reduction in fuel burned at the range for a capacity passenger and baggage load, a 2-percent greater range at this payload, and a 5-percent reduction in takeoff distance at maximum takeoff weight.

# CONTENTS

	Page
INTRODUCTION.....	1
SYMBOLS .....	5
WINGLET INSTALLATION DESIGN AND ANALYSIS .....	9
Winglet Configuration.....	9
Structural Design Criteria .....	11
Flight Loads Prediction .....	11
Structure Description .....	12
Stress Analysis.....	13
Flutter Analysis.....	13
WINGLET MANUFACTURE.....	15
AIRCRAFT PREPARATION AND WINGLET INSTALLATION.....	19
FLIGHT PROGRAM.....	21
Test Approach .....	21
Test Conditions.....	21
Aerodynamics .....	21
Structural and Aerodynamic Damping (Flutter).....	22
Loads Measurement .....	23
Flight Instrumentation .....	23
Flight Data System .....	24
Preflight Ground Tests.....	24
Ground Vibration Test .....	24
Strain Gauge Calibration Tests.....	24
Flight Test Program .....	24
RESULTS AND DISCUSSION .....	25
Baseline Phase .....	25
Basic Winglet Phase .....	25
Ground Vibration Test .....	25
Flight Test Program .....	25
Flutter .....	26
Low-Speed Buffet .....	32
Low-Speed Drag .....	37
Stall Speeds and Characteristics.....	37
Cruise Performance.....	37
Cruise Buffet.....	39
Longitudinal Static Stability .....	42
Longitudinal Maneuvering Stability.....	42
Longitudinal Trim Characteristics .....	42
Static Directional Stability.....	42
Dynamic Lateral Stability (Dutch Roll).....	44

<b>CONTENTS (Continued)</b>	<b>Page</b>
Spiral Stability and Roll Performance .....	44
Loads Measurement .....	44
Reduced-Span-Winglet Phase .....	44
Flight Test Program .....	44
Low-Speed Buffet .....	47
Low-Speed Drag .....	50
Cruise Performance .....	50
IMPACT OF FLIGHT EVALUATION RESULTS ON OPERATIONAL PERFORMANCE.....	53
CONCLUSIONS .....	55
REFERENCES.....	57

## ILLUSTRATIONS

Figure		Page
1	Winglet Model Under Development in NASA Langley 8-Foot Wind Tunnel . . . .	2
2	Flight Evaluation Program Schedule . . . . .	3
3	Test Aircraft with Basic Winglet . . . . .	4
4	Test Aircraft with Reduced-Span Winglet . . . . .	4
5	Planned Winglet Geometry . . . . .	9
6	Winglet Geometry Variations from Wind Tunnel Model . . . . .	10
7	Contingency Configurations . . . . .	10
8	Winglet Installation Components . . . . .	12
9	Basic Winglet Structural Configuration . . . . .	13
10	Predicted Flutter Speed Versus Wing Fuel — Basic Winglet . . . . .	14
11	Winglet Spar Machining . . . . .	15
12	Trailing Edge Assemblies . . . . .	16
13	Upper Winglet Assembly . . . . .	16
14	Lower Winglets . . . . .	17
15	Winglet and Wing Box Extension Assembly . . . . .	17
16	Winglet Installation in Progress . . . . .	19
17	Winglet Installation Complete . . . . .	20
18	Flight Test Program . . . . .	21
19	Ground Vibration Test Results . . . . .	25
20	Configuration Identification for Basic Winglet Flight Program . . . . .	27
21	Basic Winglet Configuration Features . . . . .	29
22	Basic Winglet Configurations with Vortilets . . . . .	30
23	Frequency and Damping Characteristics — 3 Hz Mode (Determined from Wing Tip Normal Acceleration) . . . . .	31
24	Frequency and Damping Characteristics — 4.5 Hz Mode (Determined from Winglet Longitudinal Acceleration) . . . . .	31
25	Winglet Flow in Low-Speed Flight — Inboard (Suction) Side, $C_L = 1.5, V/V_{s_{MIN}} = 1.2$ . . . . .	32
26	Winglet Flow in Low-Speed Flight — Outboard (Pressure) Side, $C_L = 1.5, V/V_{s_{MIN}} = 1.2$ . . . . .	33
27	Summary of Low-Speed Buffet Characteristics — Basic Winglet . . . . .	35
28	Low-Speed Drag Improvement — Basic Winglet . . . . .	37
29	Cruise Drag Improvement — Basic Winglet . . . . .	38
30	Basic Winglet Pressure Distribution at Cruise . . . . .	40
31	Effect of Lower Winglet on Basic Upper Winglet/Wingtip Pressure Distribution at Cruise . . . . .	41
32	Effect of Basic Winglet on High-Speed Buffet Boundary . . . . .	42
33	Effect of Basic Winglet on Longitudinal Static Stability . . . . .	43
34	Effect of Basic Winglet on Longitudinal Maneuvering Stability . . . . .	43

## ILLUSTRATIONS (CONTINUED)

Figure		Page
35	Configuration Identification for Reduced-Span Winglet Flight Program .....	45
36	Reduced-Span Winglet Configurations .....	46
37	Summary of Low-Speed Buffet Characteristics — Reduced-Span Winglet .....	48
38	Buffet Response Acceleration Power Spectra .....	49
39	Low Speed Drag Improvement — Reduced-Span Winglet .....	50
40	Cruise Drag Improvement — Reduced-Span Winglet .....	51
41	Effect of Configuration Variables on Cruise Drag Improvement — Reduced-Span Winglet .....	52
42	Increases in Operator's Empty Weight .....	53
43	Effect of Winglets on DC-10 Series 10 Performance Characteristics .....	54
44	Effect of Winglet Configurations on Fuel Burned .....	54

## INTRODUCTION

One of the technological advances to be considered for energy savings for transport application is the winglet concept developed by Dr. R. T. Whitcomb of the National Aeronautics and Space Administration (Reference 1). The winglet is an airfoil surface mounted almost vertically at an airplane's wing tip. It is intended to reduce lift-induced drag, which accounts for as much as 40 percent of the total drag at cruise speed. Historically, one of the primary ways of reducing this drag has been to increase the wing span, but this results in a heavier wing structure and so dilutes the performance gain. The concept of the winglet is to achieve the same drag reduction as with the wing-tip extension but with less penalty on the wing bending moment.

A substantial amount of wind tunnel and flight testing has been conducted on winglets since the original NASA Whitcomb experiments. Significant performance gains have been demonstrated in the NASA/USAF flight program with the KC-135, which is representative of a large first-generation jet transport aircraft, and with other smaller aircraft. However, application to a representative second-generation jet transport, such as the DC-10, was recognized as needing further investigation, primarily due to the differences in wing design.

Second-generation wings tend to be less tip-loaded and therefore do not offer the potential for induced-drag reduction provided by a wing-tip device. Also, they incorporate advanced high-lift devices resulting in significantly higher lift coefficients in the low-speed regime. Such high loadings afford greater potential for low-speed drag reduction but introduce the possibility of adverse viscous effects on winglet performance. The distinction of high loading also separates the typical large transport application from some current production corporate aircraft.

Under the Energy Efficient Transport (EET) project, investigations were therefore conducted to build the technology for the DC-10-type aircraft. Results of the initial EET high-speed wind tunnel test (Reference 2) were used to develop a satisfactory configuration and identify the cruise performance benefit. The development work was done on a DC-10 Series 10 model, and established a configuration having a large upper winglet and small supplementary lower winglet, as shown in Figure 1. Additional evaluations were then made with the longer-wing-span Series 30 model. Subsequent model tests (Reference 3) followed with the Series 30 as a basis, the general results being applicable also to the Series 10.

In low-speed wind tunnel tests, it was evident that the flow separation on the upper winglet occurred at high incidence as the critical climb condition was approached. With a winglet leading edge slat installed, the separation was delayed, but with little effect on the drag reduction. This test program, together with a high-speed test, also investigated the aerodynamic stability and control characteristics of the aircraft, and found them to be little affected by winglets. In parallel, investigations of the dynamic behavior of this winglet aircraft were made. Previous

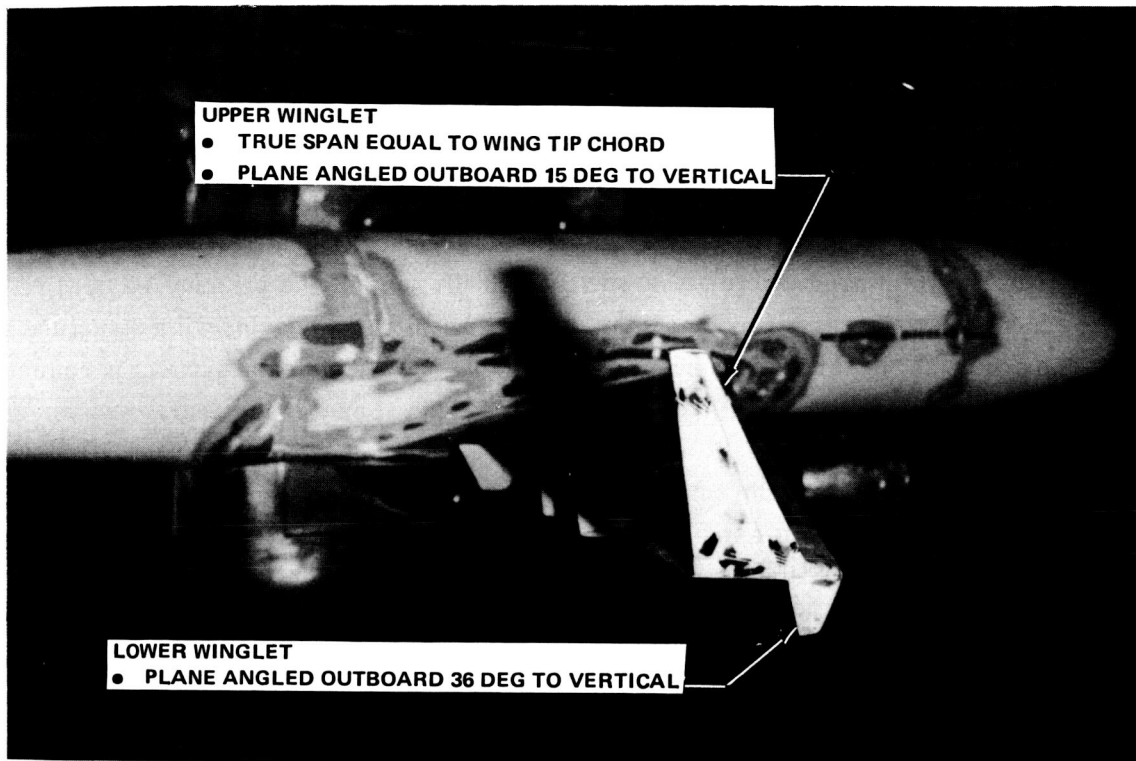


**FIGURE 1. WINGLET MODEL UNDER DEVELOPMENT IN NASA LANGLEY 8-FOOT WIND TUNNEL**

concern as to the effects of winglets on flutter was somewhat alleviated by the low-speed model investigations in which good correlation was shown with analyses using modern methods.

The configuration data resulting from these investigations and parallel work conducted at Douglas were generated by model experiments and analyses; from them it was decided that the logical next step in development was full-scale flight evaluation.

The objectives of the flight evaluation were to determine:

- The effects of winglets on performance and flying qualities of a modern jet transport aircraft, represented in this case by the DC-10. These effects would be determined by back-to-back flights with and without winglets.
- The effects of winglets on aircraft flutter
- The effects of winglets on flight loads through back-to-back measurements (this portion of the program was sponsored by Douglas).

In addition to the basic winglet (BWL) derived from the wind tunnel tests, the program tested a reduced-span winglet (RSWL) so that the effects of upper winglet span could be studied.

The flight evaluation program was conducted on a DC-10 aircraft supplied by Douglas. The aircraft was leased from Continental Airlines and was returned to airline service after the program. The program consisted of detail design, winglet manufacture, aircraft preparation (including modification of the wing structure), winglet installation, ground and flight testing, and aircraft refurbishment for delivery to airline service. The flight testing was structured so that key data comparisons between the baseline aircraft without winglets and the winglet-equipped aircraft were obtained from back-to-back test phases. The baseline test program involved 12 flights and the winglet program 49.

Baseline flights, and the winglet first flight, were made from the Douglas Long Beach facility. The winglet flutter testing was conducted from Edwards Air Force Base. Subsequent winglet flight tests were made from the Douglas facility at Yuma, Arizona.

The predominant parts of the flight test program concerned performance measurement to obtain the drag reduction due to winglets, and the development of configurations with satisfactory low-speed characteristics. The program, from inception of design through manufacture, test, and refurbishment of the test aircraft, was accomplished in 16 months. The program schedule is shown in Figure 2.

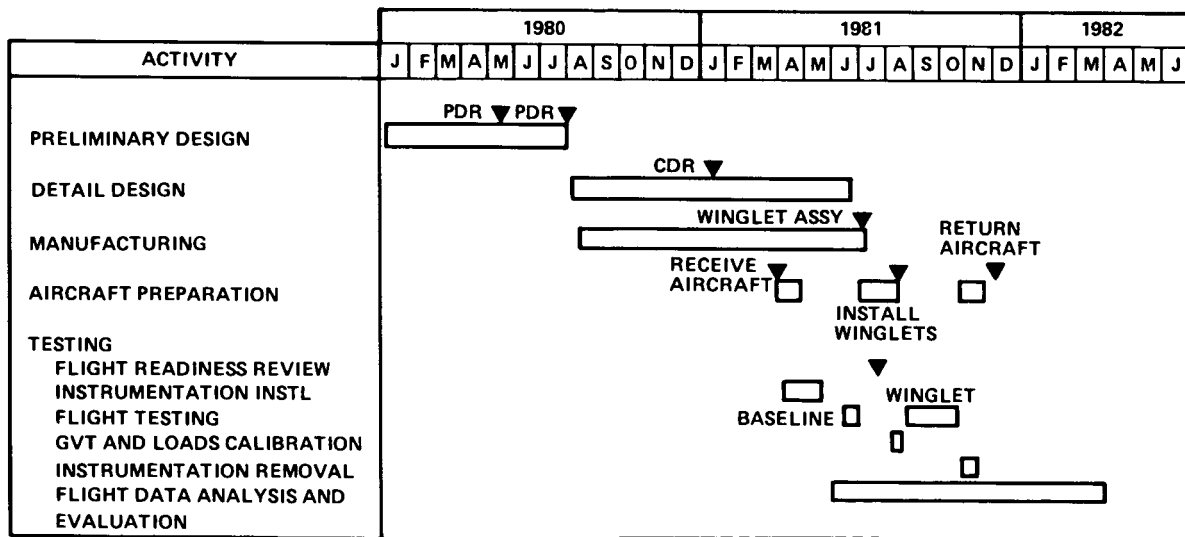


FIGURE 2. FLIGHT EVALUATION PROGRAM SCHEDULE

The test aircraft equipped with the BWL is shown in flight in Figure 3. The aircraft with the RSWL is shown in Figure 4.

The flight evaluation contract program is reported fully in Reference 4.



**FIGURE 3. TEST AIRCRAFT WITH BASIC WINGLET**



**FIGURE 4. TEST AIRCRAFT WITH REDUCED-SPAN WINGLET**

## SYMBOLS

Principal measurements and calculations were in customary units and were converted to the International System of Units (SI) for this document.

AIC	aerodynamic influence coefficient
BWL	baseline winglet
$C/C_c$	damping ratio (where $C_c$ is the critical damping)
$C_D$	drag coefficient
$C_L$	lift coefficient
$C_{L_{\text{Buffet}}}$	buffet lift coefficient
$C_p$	pressure coefficient
CG, cg	center of gravity
CDR	Critical Design Review
C of A	certificate of airworthiness
CONFIG	configuration
EET	Energy Efficient Transport project, a number of tasks sponsored by NASA under the Aircraft Energy Efficiency program to expedite development in aerodynamics and active controls
$F_{cc}$	control column force
FAA	Federal Aviation Administration
FAR	Federal Aviation Regulation (Part 25: Airworthiness Standards, Transport Category Airplanes is mentioned in this report)
G	vibratory acceleration normalized to gravity
GVT	ground vibration test

## SYMBOLS (CONTINUED)

$g$	acceleration due to gravity
LE	leading edge
LH	left hand
$M, M_N, M_0$	free-stream Mach number
MAC	mean aerodynamic chord
MTOGW	maximum takeoff gross weight
MZFW	maximum zero fuel weight
OEW	operator empty weight
PDR	Preliminary Design Review
RFD	refurbish for delivery
RMS	root mean square
RSWL	reduced span winglet
$V$	aircraft velocity
$V_D$	dive speed
$V_S$	stall speed
$V_{MIN}$	FAA-certified stall speed
$V_2$	takeoff safety speed
$\delta_F$	wing flap setting angle in degrees. An angle of zero may be associated with a retracted leading edge slat (denoted as O/RET) or with the slat extended to takeoff position (O/EXT). Other angles used in this report and with takeoff slats were 15 degrees (15/EXT) and 22 degrees (22/EXT). A 50-degree angle was also used, in this case the slat being extended fully to the landing position (50/LND).

## SYMBOLS (CONTINUED)

$\Delta$	delta
$\eta$	span ratio, percent

# WINGLET INSTALLATION DESIGN AND ANALYSIS

## Winglet Configuration

The planned configurations of the basic winglet (BWL) and the reduced-span winglet (RSWL) are shown in Figure 5. The BWL configuration was directly related to the original designs developed by Dr. R. T. Whitcomb of NASA Langley (Reference 1). The specific design for the DC-10 was developed in the initial EET project wind-tunnel tests (Reference 2), with minor changes made as the result of subsequent tests (Reference 3). In addition, the flight test configuration for the DC-10 Series aircraft included modifications to allow for the existing wing tip position lights. The changes in the flight configuration from the developed configuration of Reference 2 are shown in Figure 6. The flight configuration, as in the wind tunnel, was set at an incidence of  $-2$  degrees relative to the fuselage centerline. The lower winglet was set at zero incidence. Neither surface was twisted.

Certain contingency provisions were included in the winglet design. These are illustrated in Figure 7, and consist of a bolt-on leading-edge device for the upper winglet and a provision to move the lower winglet forward or remove it altogether. As a result of the high-lift wind tunnel

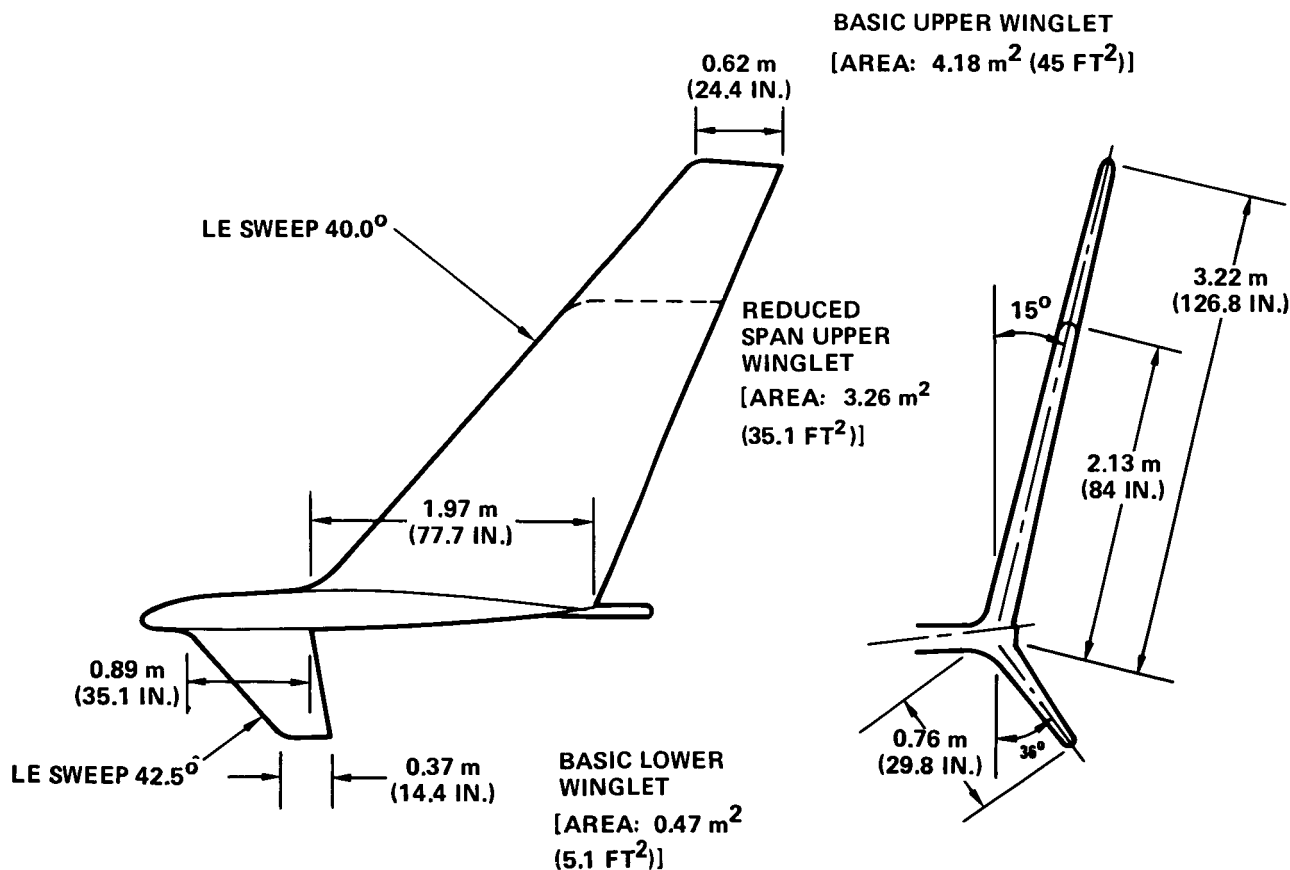
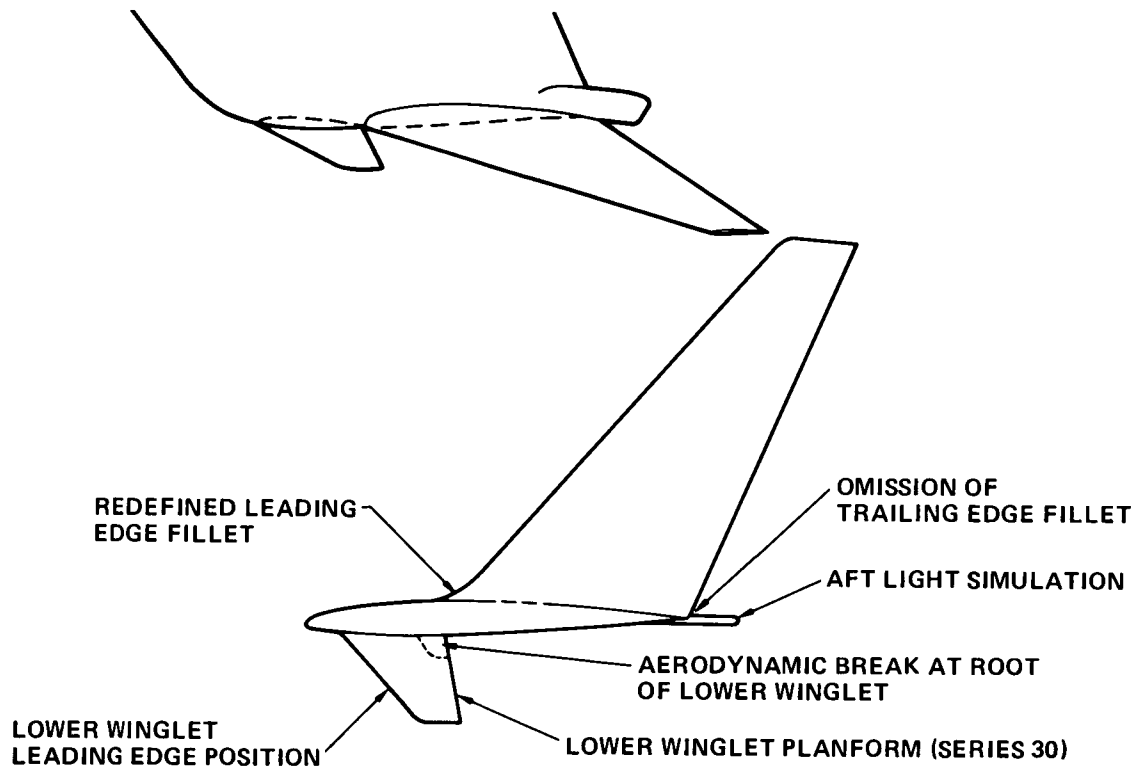
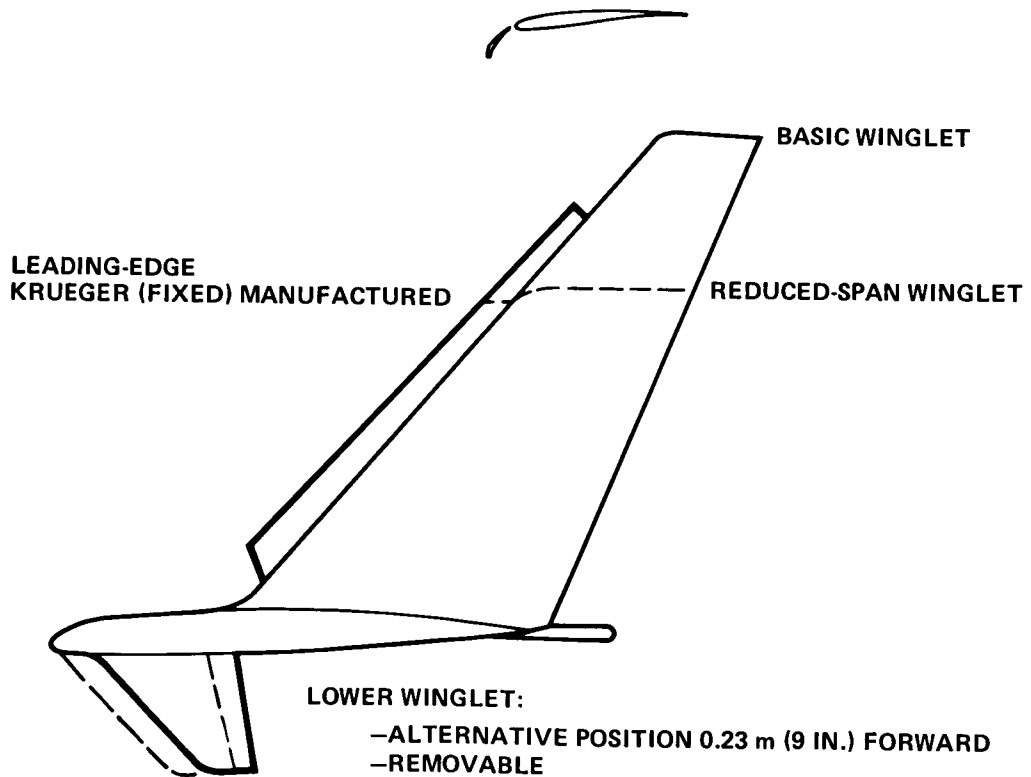


FIGURE 5. PLANNED WINGLET GEOMETRY



**FIGURE 6. WINGLET GEOMETRY VARIATIONS FROM WIND TUNNEL MODEL**



**FIGURE 7. CONTINGENCY CONFIGURATIONS**

tests, it was considered prudent to have a leading-edge device available for installing on the winglet should the need arise. The additional contingency provision was made to enable the exploration of the effect of lower winglet position or absence on flow interference between upper and lower winglets.

### **Structural Design Criteria**

The test aircraft configuration was derived from the baseline aircraft definition and the test conditions described later in this report. It was determined that the test objectives could be met using aircraft speeds, gross weight, center of gravity, and load factor lower than the maximum certified. These limitations minimized the modifications to the wing structure that were to remain with the aircraft on its return to airline service. The test aircraft limitations chiefly included maximum Mach number of 0.91, maximum gross weight of 181 437 kg (400,000 lb), and maneuver load factor of 2.0.

FAR Part 25 static strength requirements (2.5g limit) governed the design of the winglet and its attachment to the wing, thus providing substantial margins of safety in the new structure. Design-level gust intensities for clear-air turbulence were included in the design. Specific criteria were applied to the design of the winglet so that aerodynamic data quality was preserved in the presence of flight deflections.

Fatigue was not a consideration for the winglet flight test phase having regard to the limited flight test time; however, satisfactory fatigue life of the aircraft as refurbished for delivery was assured.

### **Flight Loads Prediction**

Winglet loads were estimated using a combination of theoretical and wind tunnel test data. The resulting forces and moments were then applied to existing aeroelastic models of the wing structure to estimate the external loads. In addition, the influence of the winglet on the wing spanwise lift distribution was estimated.

The main component of force on the winglet is the normal force. The force coefficients used for design employed a composite of linear and nonlinear wind tunnel test data, together with analytical corrections. Initially, data linearly extrapolated from limited test data were used. Later, wind tunnel data over a more extensive range suggested higher loads at low angle of attack and lower loads at the higher angles. For conservatism in design, an envelope of the data was employed.

## Structure Description

The structure which was designed for the tests consisted of an upper winglet, a lower winglet, and a wing box extension attached to the test aircraft wing box at the outer fuel-closure bulkhead (Figure 8). In addition, the wing box upper skin panels were strengthened.

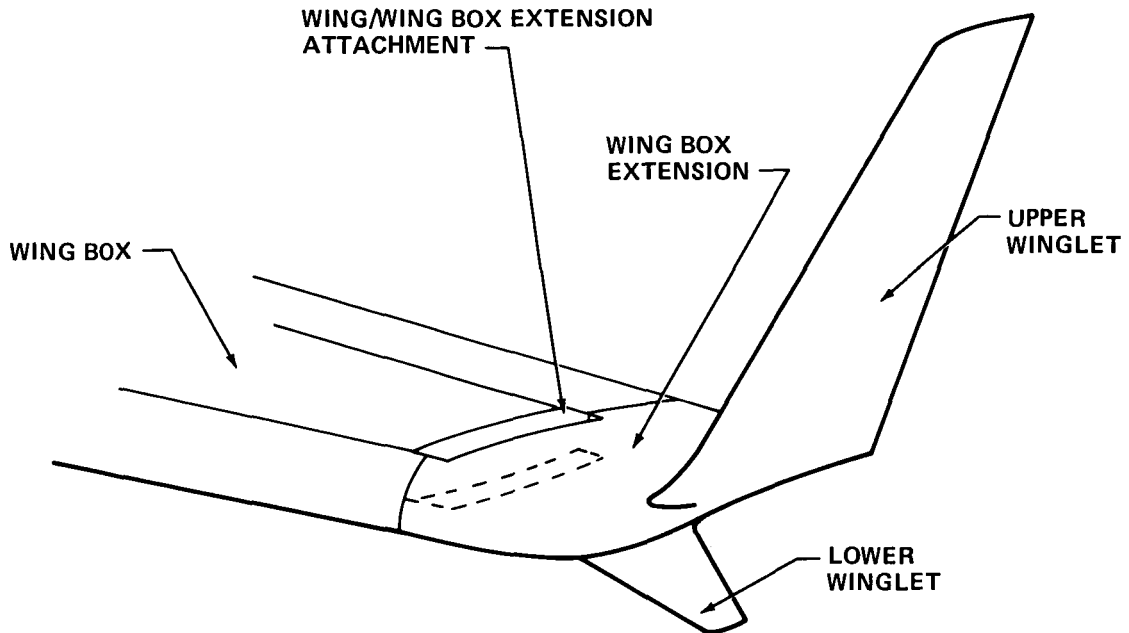
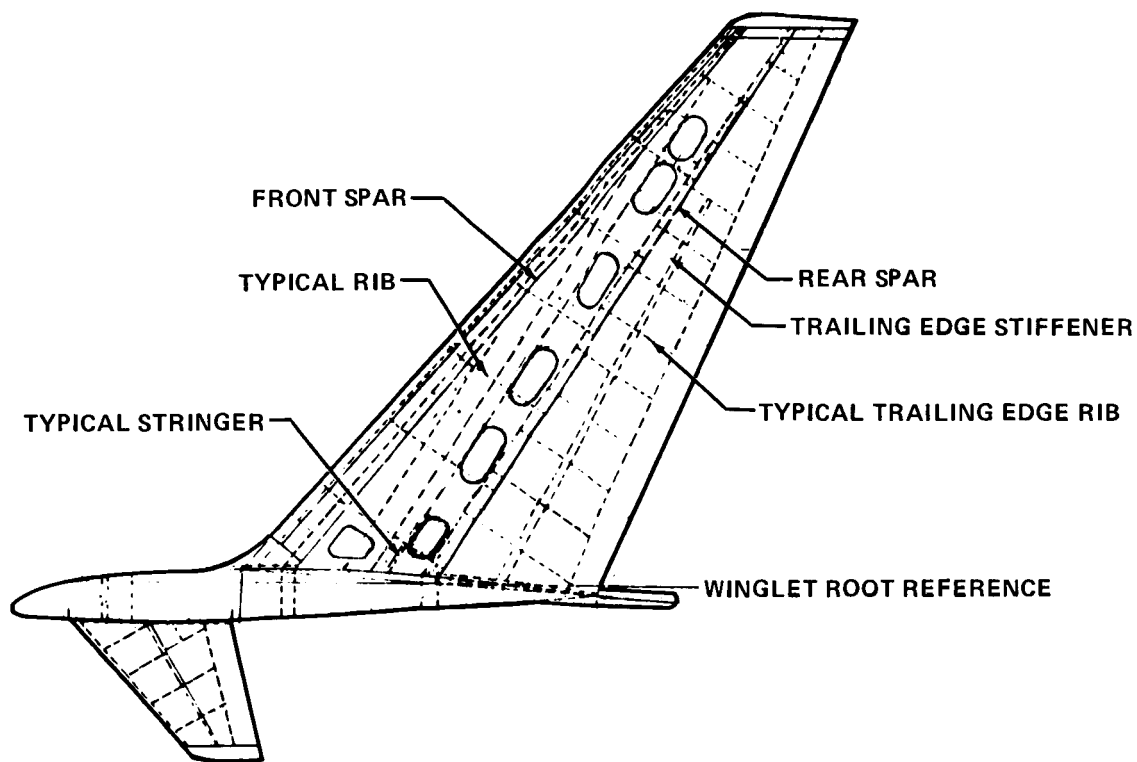


FIGURE 8. WINGLET INSTALLATION COMPONENTS

The winglet structure is shown in Figure 9. The upper winglet was designed with a primary structure of conventional metal construction having two spars with skins and ribs. The wing box extension spars were continuous with those of the upper winglet, with the rear member spliced to the wing rear spar across the fuel bulkhead. The new extension, also having conventional aluminum structure with skins and ribs, was further attached to the wing skins, stringers, and fuel-closure bulkhead through external splice plates and internal fittings. The fairing of the juncture between the upper winglet and the wing box extension was merged aft with a fairing representing the trailing edge position light installation. Each lower winglet used a single aluminum spar with glass-fiber/epoxy laminate skins. This material was also used for the leading and trailing edges of the upper winglets, and similar secondary structure. Conversion from BWL to RSWL was done in the field by cutting through the entire structure at the appropriate spanwise station. A new winglet tip was installed at that time.

The wing was strengthened by reinforcing the upper wing panel stiffeners with angle members. The reinforcing affected approximately 7.6 m (300 in.) inboard of the wing box extension attachment. In general, the type of reinforcing was a simple angle.



**FIGURE 9. BASIC WINGLET STRUCTURAL CONFIGURATION**

The leading-edge Krueger flap, previously described, was designed and manufactured to bolt to the leading edge of the upper winglet. The flap was constructed so that the upper end could be trimmed in the field for the RSWL tests.

### **Stress Analysis**

A finite-element model was used to analyze the upper winglets, the wing box extension, and that portion of the existing wing approximately four wing tip chords inboard from the tip. The inboard end of this model was joined analytically to a shell analysis used for the inboard portion of the wing.

### **Flutter Analysis**

The selection of test configurations and flight conditions to be used in the flight flutter tests was based on flutter analysis results. This analysis predicted the important vibration modes, frequencies, and flutter speed margins of the aircraft with winglet systems installed. The results of the analysis were verified later through a ground vibration test (GVT) conducted to measure the important mode shapes and frequencies.

The critical flutter mode for the basic DC-10 Series 10 without winglets is a symmetric 3-Hz mode involving coupling between first wing bending and first wing torsion. The addition of the winglets was estimated to reduce the flutter speed of the 3-Hz wing mode. In addition, the winglets introduced a 4-Hz flutter mode involving second wing bending and second wing torsion. Because of these adverse effects, 226.8 kg (500 lb) of mass balance was installed in each wing tip to ensure adequate flutter margins for flight testing.

Flutter speeds were normalized to a reference dive speed,  $V_{REF}$ , of 706 km/h (381 KEAS) which corresponds to  $M = 0.9$  on the  $M_D/V_D$  boundary. The flutter speeds for the 3- and 4-Hz modes are shown in Figure 10, the former mode showing the lower flutter speed at all fuel levels. The 4-Hz-mode flutter speed was higher than that for the 3-Hz mode, and was above  $1.2 V_{REF}$  for all fuel loadings. Based on these results, minimum fuel states for performance tests were determined.

At the time of the GVT, an additional flutter analysis was performed using measured frequencies. Slightly higher flutter speeds were obtained using the test data. For conservatism, however, theoretical modal frequencies were used for all flutter speed predictions.

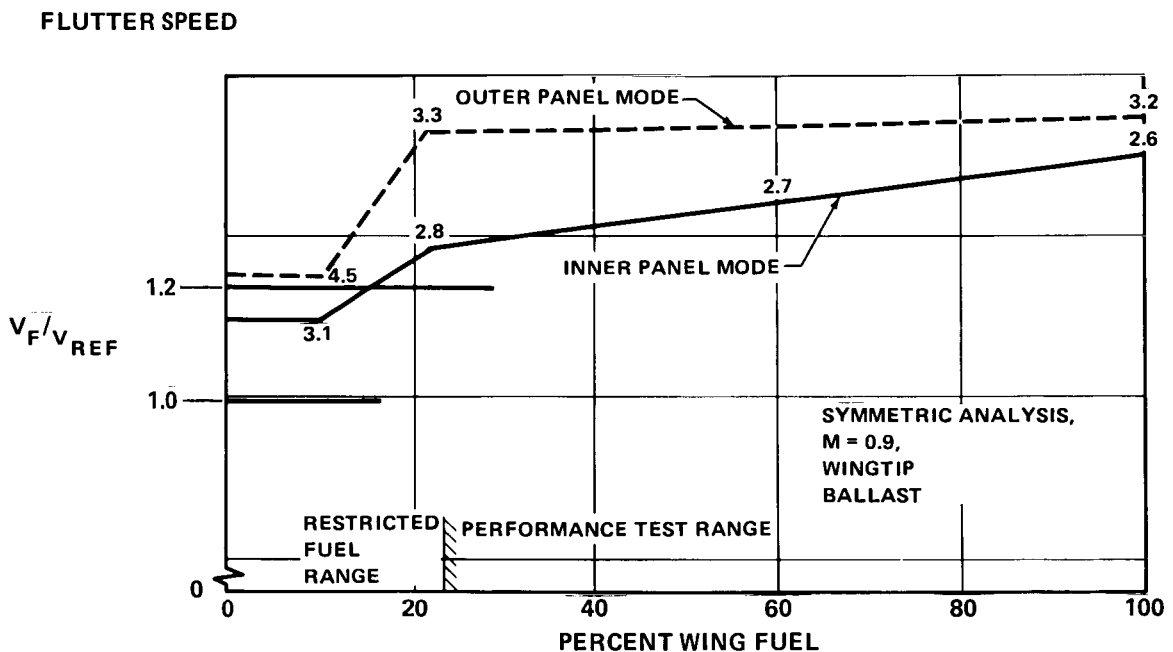


**FIGURE 10. PREDICTED FLUTTER SPEED VERSUS WING FUEL – BASIC WINGLET**

## WINGLET MANUFACTURE

The main stages of the winglet manufacture are illustrated in Figures 11 through 15. Figure 11 shows the machining of one of the upper winglet spars. This unit was machined from a hand forging using computer-aided manufacturing techniques. During machining and heat treatment, its location was determined by tabs along the length, these being removed in the final stages of fabrication. Figure 12 shows the winglet trailing edge assemblies being built on simple fixtures. The winglet spars were used essentially as locating tooling during the winglet assembly. Figure 13 shows an enclosed winglet box located in its assembly jig in position, with the trailing edge assembly attached. Two stages of lower winglet assembly are presented in Figure 14, showing the skin and rib assemblies forward and aft of the main spar. The completed assembly minus the lower winglet is shown ready for installation in Figure 15.

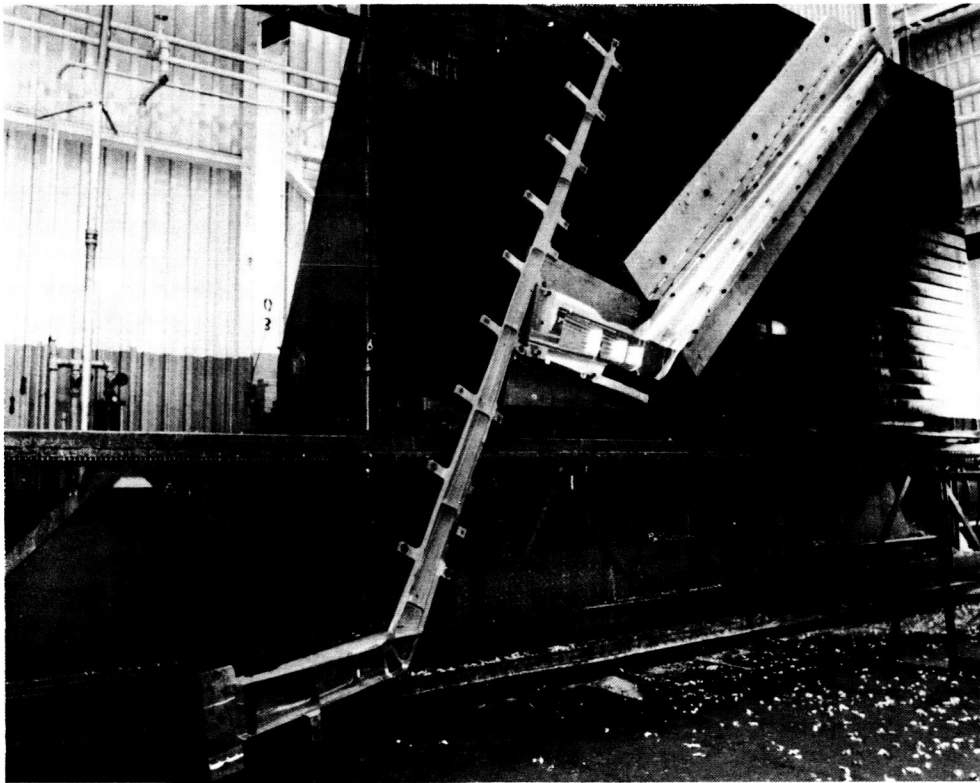
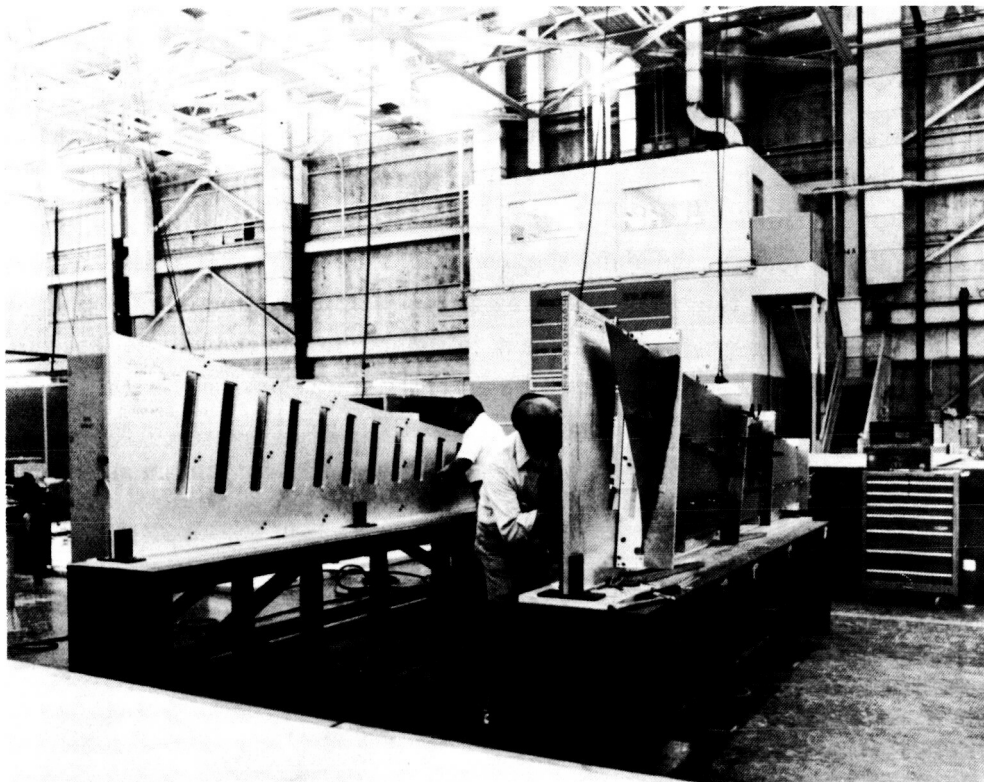
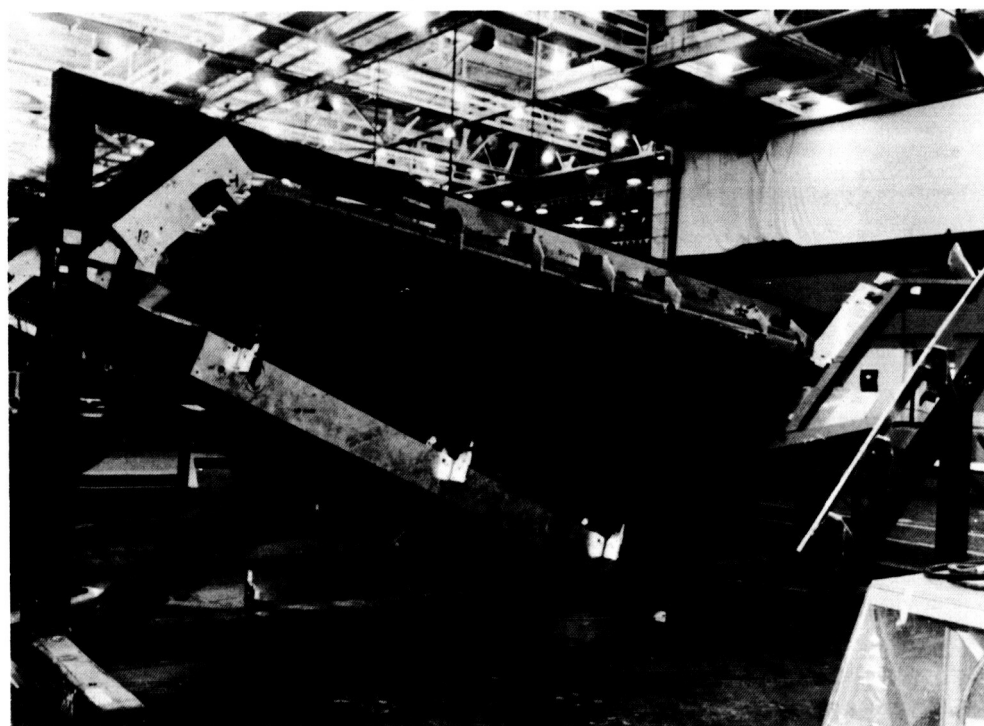


FIGURE 11. WINGLET SPAR MACHINING



**FIGURE 12. TRAILING EDGE ASSEMBLIES**



**FIGURE 13. UPPER WINGLET ASSEMBLY**

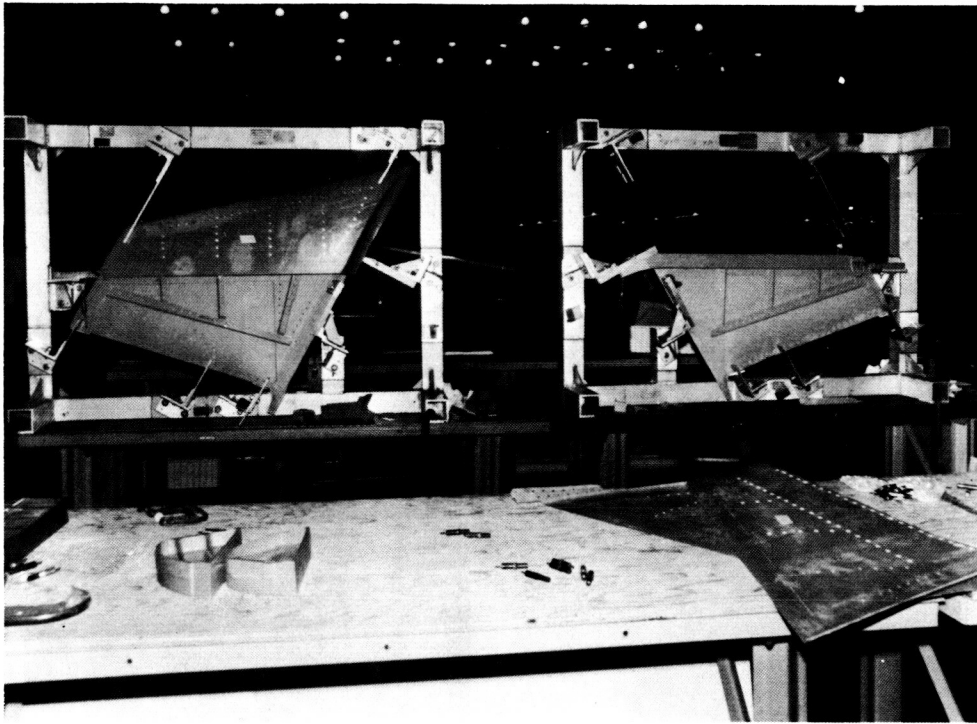


**FIGURE 14. LOWER WINGLETS**

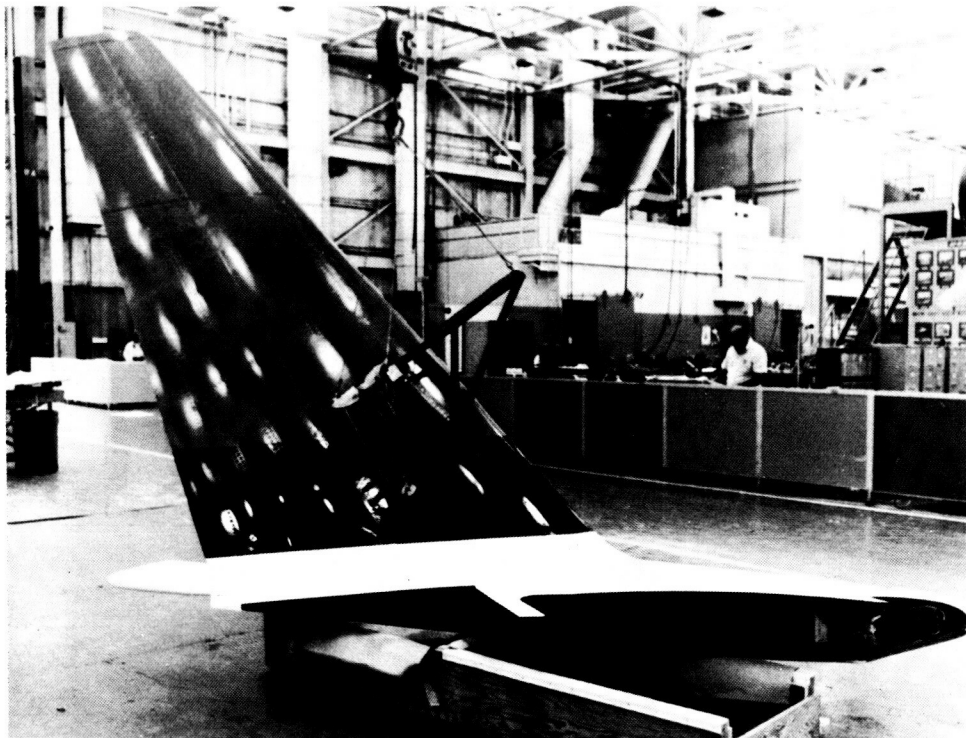


**FIGURE 15. WINGLET AND WING BOX EXTENSION ASSEMBLY**

## AIRCRAFT PREPARATION AND WINGLET INSTALLATION

The aircraft preparation phase consisted of the baseline aircraft modification, the winglet installation, and the reconfiguration for airline service after the test. The three activities were conducted in the open using simple equipment.

The modification activity primarily concerned the strengthening of the wing box. During this work, instrumentation and test equipment were installed in the aircraft. Upon completion of this activity, the baseline flight test took place.

In the second stage, the winglet assemblies were installed. This was accomplished using simple hoist equipment (Figure 16). The completed installation of the upper and lower winglets is shown in Figure 17. During the second stage, work to complete the instrumentation was undertaken.

After the winglet flight test, the aircraft was reconfigured to the baseline configuration with test equipment removed. The original wing tips were reinstalled and the aircraft refurbished prior to its return to airline service.



FIGURE 16. WINGLET INSTALLATION IN PROGRESS



**FIGURE 17. WINGLET INSTALLATION COMPLETE**

# FLIGHT PROGRAM

## Test Approach

In order to ensure accuracy in comparison and correlation, the flight test program was arranged to have back-to-back testing of the baseline and winglet aircraft in all key areas. The important areas for comparison were performance, stability and control, and loads. The program began with tests of the baseline aircraft, continued with BWL configuration tests, and was completed with RSWL testing. The flight test program is summarized in Figure 18.

	BASELINE		WINGLET	
			BWL	RSWL
PERFORMANCE CRUISE LOW SPEED	X X		X X	X X
STABILITY AND CONTROL	X	STEADY SIDESLIP ONLY	X	X STEADY SIDESLIP ONLY
DIAGNOSTIC DATA FLOW VISUALIZATION (TUFTS) WING DEFLECTION MEASUREMENT (CAMERA) PRESSURE MEASUREMENTS (WING) PRESSURE MEASUREMENTS (UPPER WINGLET)	X X		X X X X	X X X X
STRUCTURAL AERODYNAMIC DAMPING			X	X ENVELOPE EXPANSION CHECK ONLY
LOADS MEASUREMENT (DOUGLAS) ADDITIONAL PRESSURE MEASUREMENT STRAIN GAUGES	X		X X	X X

**FIGURE 18. FLIGHT TEST PROGRAM**

## Test Conditions

**Aerodynamics** — Evaluations were made in the following areas:

- Drag improvement at cruise and low speed
- High-speed-buffet boundary
- Low-speed stall speeds and characteristics
- High- and low-speed stability and control characteristics.

Performance evaluation data were obtained over typical cruise operating conditions. In addition, lower Mach numbers were flown to establish the incompressible drag. From these data

the aircraft drag coefficient was determined by obtaining the aircraft thrust required at the particular altitude and airspeed.

Buffet onset data were determined for the baseline and BWL aircraft during wind-up turns at high cruise Mach numbers measuring normal acceleration. The RSWL was only to be evaluated for buffet characteristics if a significant impact was determined from the preceding BWL tests.

Minimum stall speeds for the baseline and BWL aircraft were evaluated at conditions typical of takeoff and landing. During these tests, evidence of any buffet limitations was sought by use of accelerometer measurements in the cockpit and cabin and on the winglet. It was intended that, should unacceptable buffet be encountered, a fixed leading edge device would be attached to the upper winglet leading edge and its effect measured.

Of the two winglet configurations, stall characteristics were required only for the BWL. The need for stall characteristic tests for the RSWL was considered a contingency only in the unlikely event that the BWL showed a significant effect.

Low-speed drag polars are obtained for the baseline aircraft and for both winglet configurations by tests at the same flap settings.

Stability and control (S&C) tests primarily concerned investigation of the DC-10 with the BWL. The choice of this configuration was based on wind tunnel test results which indicated that the impact of winglets on S&C characteristics should be small. Therefore, in order to ensure quantifiable results for winglet increments in S&C parameters, the larger winglet was employed. An exception was the testing of static directional stability conducted on the baseline and both winglet configurations.

To evaluate the effects of winglets, flow visualization, estimation of wing deflection and twist, and measurement of pressures were conducted.

**Structural and Aerodynamic Damping (Flutter)** — The BWL was evaluated at the minimum fuel state for performance testing and at the flutter-critical fuel state. The latter condition required testing first at high altitude, then at medium altitude. It was originally intended that envelope clearance would also be accomplished with RSWL. As explained in the discussion on results, this test was later considered unnecessary.

Specific measurements of frequency and damping were made using accelerometers. Damping values were obtained from time histories of the transient decay of excited modes. Modal excitation was made by pilot-induced inputs to the flight controls.

**Loads Measurement** — The primary test objectives were to determine the impact of the winglet on wing loads, and the winglet load itself. In addition, the flight loads were monitored for potentially critical maneuvers.

The flight test measurements were made in a number of angle-of-attack surveys at a range of Mach numbers and load factors. Steady state yawing maneuvers were included so the effect of sideslip could be evaluated. High lift data were also included.

### **Flight Instrumentation**

The flight instrumentation consisted of the existing (production) air data computer (ADC), an additional flight test ADC and inertial system, onboard monitoring equipment including a computer, pressure orifices and strain gauges, accelerometers, and visual aids.

Owing to the back-to-back nature of the performance test, thrust-instrumented and calibrated engines were not required. However, air data and engine parameters were carefully measured.

Buffet onset characteristics were obtained from cockpit, cabin, and wing accelerometers. In order to measure the buffet response in the stall tests, additional accelerometers were installed on the empennage. Pressure distribution measurements were obtained on the right outer wing and upper winglet.

Tufts were used to determine airflow on the left winglet and wing tip. The tufts were viewed from the DC-10 cabin and a chase aircraft. Photographs of wing-mounted targets were used to obtain wing deflection data. As described in the test results discussion, the camera data were subject to error, and deflection information was obtained from loads measurements.

The flutter instrumentation consisted of accelerometers located in the winglets, wing tips, starboard wing engine, horizontal and vertical stabilizers, and captain's seat.

Control surface position instrumentation was also used. Data from the structural aerodynamic damping tests were telemetered, and were recorded onboard. The test flights were monitored from a chase airplane supplied by NASA Dryden.

The load instrumentation consisted of strain gauges and pressure measurement instruments on the wing and upper winglet. Calibrated strain gauges were installed in the winglet near its root. Uncalibrated strain gauges were installed in the wing at three spanwise positions, their readings being used in back-to-back comparisons with winglet on and winglet off. The winglet-off condition was related to previously available data.

## **Flight Data System**

The flight data system, using the Douglas facilities, enabled the test aircraft to link with the operating base at Yuma and the flight test center at Long Beach. The system provides direct output of data in engineering units, and real time data presentation, using telemetry and microwave transmission.

## **Preflight Ground Tests**

**Ground Vibration Test (GVT)** — Prior to the BWL flight tests, a GVT was conducted to measure the important mode shapes and frequencies of the test aircraft with the BWL installed. In addition, the amplitude and phases of the aircraft extremities were measured. From the test data, first the modal damping and then the normalized modal deflection and node lines were calculated.

**Strain Gauge Calibration Tests** — Calibration tests were conducted for the aileron actuator and hinge bracket and winglet root gauges. Correlation with prediction was excellent.

## **Flight Test Program**

The baseline flight test program was conducted from Long Beach, and consisted of 11 flights after the delivery flight from Continental Airlines. These flights were primarily devoted to cruise and low-speed performance.

The BWL test phase began with a general handling and envelope expansion flight. Operating from Edwards Air Force Base, the envelope expansion and structural and aerodynamic damping tests were completed. Chase plane support of this phase was provided by the NASA Dryden Flight Research Center. The subsequent test program was conducted from the Douglas test facility at Yuma, Arizona. During the first flight, low-speed buffet was observed. As a result, development activity was introduced into the program aimed at identifying and resolving the problem. BWL program objectives were accomplished in all essentials.

Upon completion of the BWL phase, the upper winglet span was reduced for the RSWL testing. Owing to the results and quantity of data obtained in the preceding phase, the previously planned envelope expansion test was eliminated. For the same reason, other changes to the originally planned program were made. In particular, a test was added to measure the effect of drooping the outboard ailerons. RSWL phase objectives were met in all essentials.

## RESULTS AND DISCUSSION

### Baseline Phase

The planned objectives for the baseline phase were achieved, and a basis for comparing the results of the winglet program was established.

### Basic Winglet Phase

**Ground Vibration Test** — The frequencies obtained in the test results are summarized, and compared with the theoretical modal frequencies, in Figure 19. In general, the agreement is good except for the symmetric and antisymmetric first wing bending modes and the higher frequency modes involving winglet flexibility. The first wing bending frequencies were affected significantly by the support system stiffness. As previously noted, the use of measured data in a revised flutter analysis led to a higher flutter speed capability than formerly predicted. For conservatism, the lower estimated figure was used as the basis for the flight program.

**Flight Test Program** — The planned objectives for this phase were achieved. In addition, the development activity, which was primarily due to the low-speed buffet investigation, was inserted into the program. Two of the three contingency configurations, applying the leading edge Krueger flap and removing the lower winglet as shown earlier in Figure 7, were employed.

EMPTY FUEL  
BASIC WINGLET  
AIRCRAFT ON SUPPORT SYSTEM

	MODE DESCRIPTION	FREQUENCY, Hz		PERCENT DIFFERENCE
		THEORY	MEASURED	
SYMMETRIC MODES	FIRST WING BENDING	1.73	1.61	7.4
	WING ENGINE YAW	1.98	1.95	1.5
	WING ENGINE PITCH WITH WINGLET IN PHASE	3.40	3.23	5.3
	WING ENGINE PITCH WITH WINGLET OUT-OF-PHASE	3.83	3.82	0.3
	HORIZONTAL STABILIZER BENDING	4.21	4.10	2.7
	WING FORE AND AFT BENDING WITH WINGLET IN PHASE	5.05	4.64	8.8
	WING FORE AND AFT BENDING WITH WINGLET OUT-OF-PHASE	5.30	5.46	-2.9
	ANTISYMMETRIC MODES	WING ENGINE YAW	2.05	1.96
FIRST WING BENDING		2.48	2.21	12.2
VERTICAL STABILIZER BENDING				
HORIZONTAL STABILIZER OUT-OF-PHASE		3.56	3.27	8.8
SECOND WING BENDING WITH ENGINE PITCH		3.84	3.79	1.3
WING FORE AND AFT BENDING WITH WINGLET IN PHASE		5.24	5.05	3.7
SECOND WING BENDING WINGLET BENDING WITH WING FORE AND AFT IN PHASE		6.59	6.37	3.4
		7.31	8.20	-12.0

FIGURE 19. GROUND VIBRATION TEST RESULTS

All the configurations tested in the BWL phase, including those added in the development activity, are described in Figure 20. The rationale for the added configurations is included in a subsequent discussion. In this figure, Configuration 1 is the original BWL, Configuration 2 is Configuration 1 with the Krueger flap fitted, and Configuration 3 is Configuration 2 with the lower winglet removed. More extensive modifications were then made, the chief features of which are illustrated in Figures 21 and 22. A description of the specific configurations, consistent with that in Figure 20, follows:

- Configurations 4 and 5: Configuration 3 with Vortilet Number 1, Krueger flap angle adjustments being applied in the latter case. The term vortilet was coined to describe an upper winglet dorsal fin originating near the wing-tip leading edge and extending to a point on the winglet leading edge.
- Configurations 6 and 8: Configuration 3 with the Krueger flap extended to the winglet root (see Figure 21).
- Configuration 7: Configuration 8 with the lower winglet installed.
- Configuration 9: Configuration 1 without the lower winglet.
- Configuration 10: Configuration 1 with the addition of Vortilet Number 2 and a modified upper winglet airfoil (MOD 6). Vortilet Number 2 extends to a point on the upper winglet further outboard on its span than on Vortilet 1.
- Configuration 11: Configuration 10 without the lower winglet.
- Configuration 12: Configuration 10 with MOD 6 removed and the Krueger flap installed above the vortilet.

As the program progressed, it became clear that the eventual configuration should attempt to balance or resolve two characteristics of the original BWL which were in apparent conflict — that the lower winglet was beneficial in improving cruise performance and that the lower winglet adversely contributed to the low-speed buffet. This investigation was continued into the RSWL phase.

**Flutter** — Frequency and damping data from the Configuration 1 flutter tests are shown in Figures 23 and 24 for the 3-Hz and 4.5-Hz modes, respectively. The figures include the analytical predictions, and are for the flutter-critical condition. The test results show the frequency and damping of both modes to be relatively constant over the test speed range, with no loss of damping as 0.91 Mach number is approached. Similar trends and damping levels occurred with the remaining cases having symmetric excitation. The antisymmetric excitation conditions were more highly damped by over 1.5 percent.

The predicted subcritical frequencies closely matched the measured frequencies. For the 3-Hz mode, the predicted damping, though generally in agreement with that measured, was

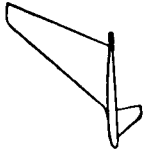
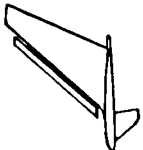
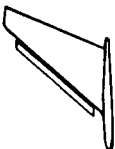
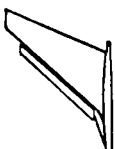
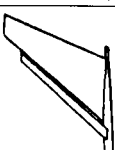
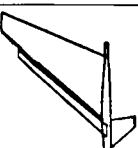
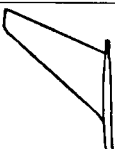
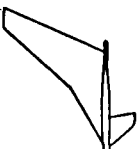
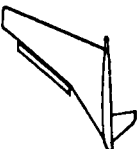
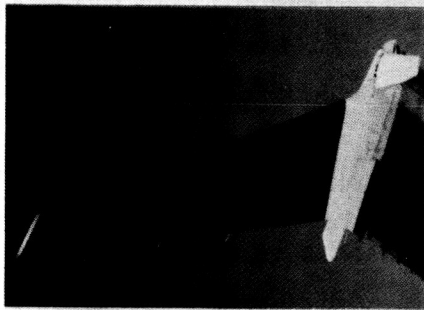
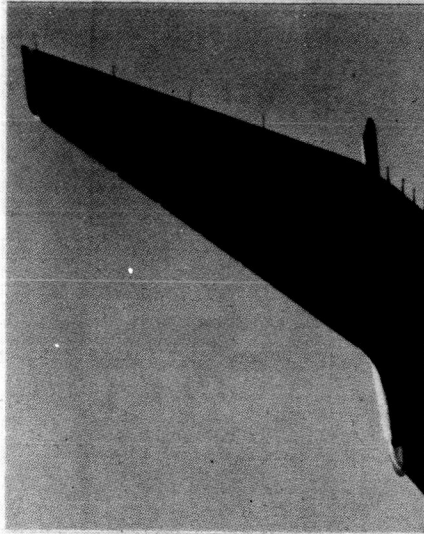
CONFIG NO.	PHYSICAL APPEARANCE	DESCRIPTION	FLIGHT NO.
1		BASIC UPPER AND LOWER WINGLET AS ORIGINALLY DESIGNED	A13-A26
2		CONFIGURATION NUMBER 1 WITH KRUEGER FLAP ATTACHED TO UPPER WINGLET WITH 50-DEGREE DEFLECTION	A27
3		CONFIGURATION NUMBER 2 WITH LOWER WINGLET REMOVED	A28
4, 5		CONFIGURATION NUMBER 3 WITH VORTILET 1 INSTALLED. VORTILET STARTED AT AFT END OF WING TIP LIGHT AND ENDED AT LOWER END OF KRUEGER FLAP	4-A29 5-A30
6, 8		BASIC UPPER WINGLET WITH KRUEGER FLAP EXTENDED TO WING TIP	6-A31 8-A33-A41
7		BASIC UPPER WINGLET WITH KRUEGER FLAP EXTENDED TO WING TIP AND DEFLECTED 40 DEGREES	A32
9		BASIC UPPER WINGLET WITH OUT LOWER WINGLET OR LEADING EDGE DEVICE	A42-A46
10		LARGE VORTILET 2 INSTALLED WHICH EXTENDED FROM AFT EDGE OF WING TIP LIGHT TO UPPER WINGLET LEAD. WING EDGE AT ABOUT 37 PERCENT SPAN. MODIFIED (DROOPED LEAD-ING EDGE) AIR-FOIL ABOVE VORTILET 2. BASIC LOWER WINGLET INSTALLED	A47
11		CONFIGURATION NUMBER 10 WITHOUT WINGLET	A48
12		CONFIGURATION NUMBER 10 WITH MODIFIED AIRFOIL RE-MOVED AND KRUEGER FLAP INSTALLED ABOVE VORTILET 2	A49

FIGURE 20. CONFIGURATION IDENTIFICATION FOR BASIC WINGLET FLIGHT PROGRAM



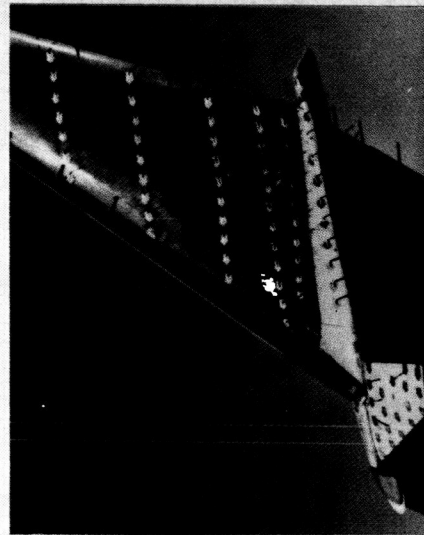
10.6-FOOT UPPER WINGLET  
AND 2.5-FOOT LOWER WINGLET



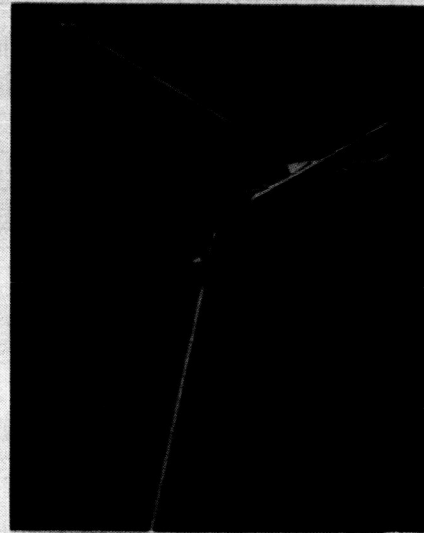
10.6-FOOT UPPER WINGLET  
WITHOUT LOWER WINGLET



WING TIP LIGHT FAIRINGS



UPPER WINGLET KRUEGER FLAP

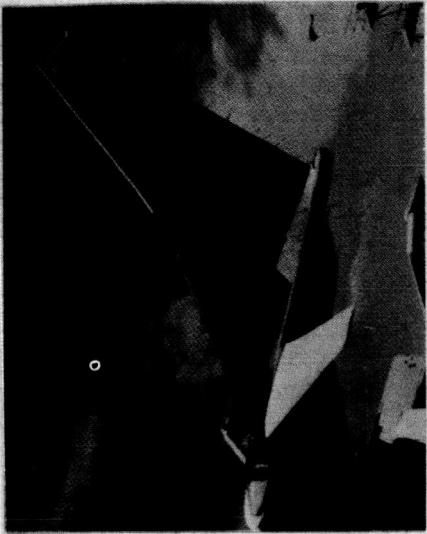


UPPER WINGLET KRUEGER FLAP



KRUEGER FLAP EXTENSION  
TO WING TIP

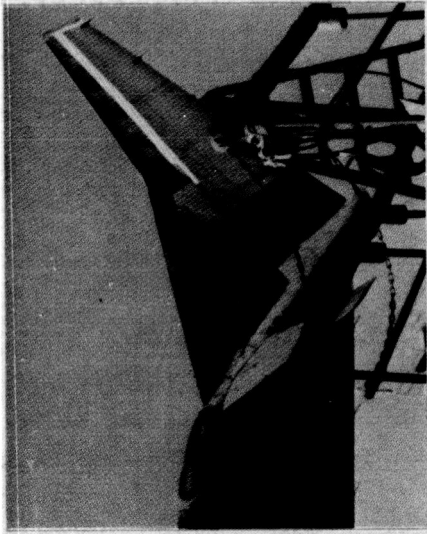
FIGURE 21. BASIC WINGLET CONFIGURATION FEATURES



VORTILET NO. 2 WITH SHORTENED KRUEGER FLAP



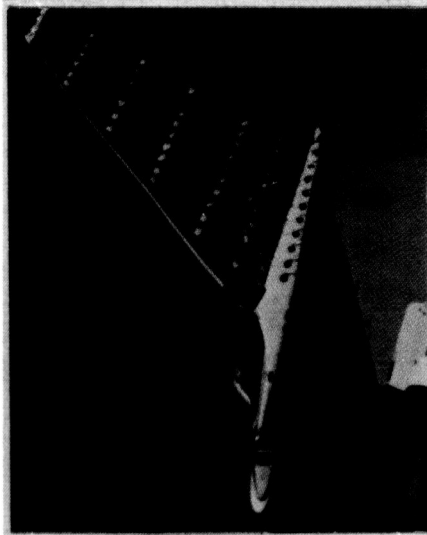
VORTILET NO. 2 WITH SHORTENED KRUEGER FLAP



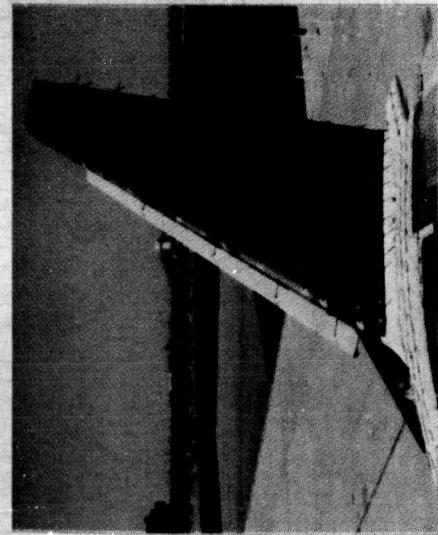
VORTILET NO. 2 WITH MOD 6



VORTILET NO. 2 WITH MOD 6



OUTBOARD VIEW OF VORTILET NO. 1



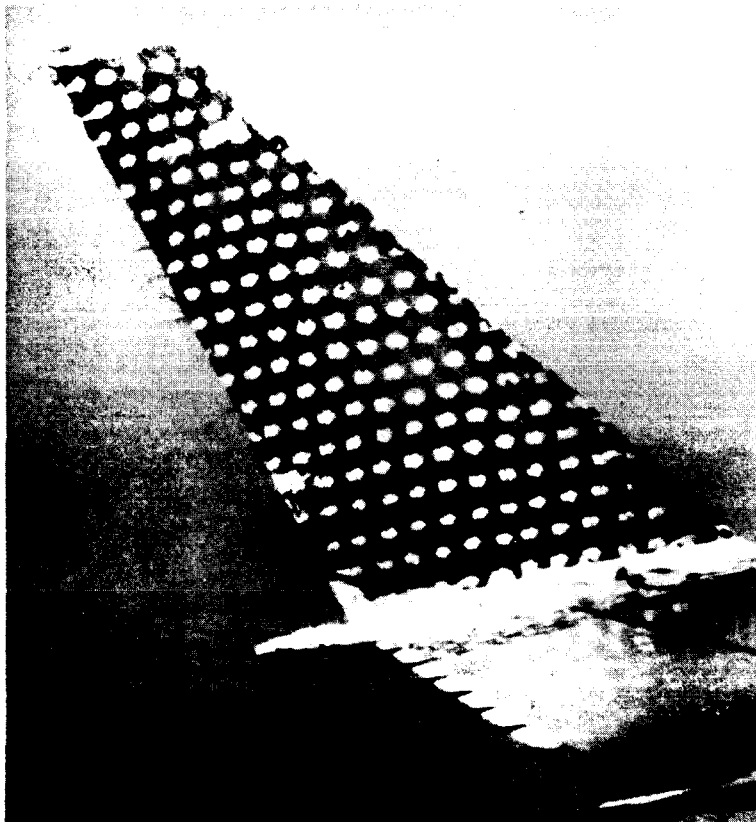
INBOARD VIEW OF VORTILET NO. 1

FIGURE 22. BASIC WINGLET CONFIGURATIONS WITH VORTILETS



slightly less than the measured damping at the higher Mach numbers and therefore conservative. For the 4.5-Hz mode, the predicted damping was higher than that measured and therefore unconservative. An estimate of this effect shows the flutter speed to still be over  $1.2 V_D$ .

**Low-Speed Buffet** — The planned early assessment of any potential low-speed problem was made since wind tunnel investigations (Reference 3) had indicated the possibility of flow separation prior to wing stalling. During the flight test with Configuration 1, buffet occurred during the critical takeoff and landing conditions of  $1.2 V_{MIN}$  and  $1.3 V_{MIN}$ , respectively. Flow observations indicated that the buffet corresponded to a completely separated flow on the suction side of both the upper and lower winglets. The flow separation developed gradually. At lifting conditions corresponding to  $1.5 V_{MIN}$ , where there was no buffet, the upper winglet had no separated flow, although the flow on the lower winglet was about 70-percent separated. At  $1.2 V_{MIN}$ , an unacceptable buffet was felt in the cockpit. The buffet was characterized by a strong vertical bounce component, which according to the pilot would make the aircraft uncertifiable. The flow patterns observed were similar to those obtained in the wind tunnel tests, except that in the wind tunnel the separation occurred at higher lift coefficients. The extent of the flow separation at  $1.2 V_{MIN}$  is shown in Figures 25 and 26. As a result of these findings from the assessment flight, an extensive effort was undertaken to find a configuration with acceptable buffet characteristics.



**CONFIGURATION**

- BASIC UPPER WINGLET WITH LOWER WINGLET
- NO LEADING-EDGE DEVICE
- $\delta_F = 15 \text{ DEG}$
- $\delta_S = \text{TAKEOFF}$

WINGLET FLOW SEPARATED.  
SEPARATION CARRIES OVER TO  
WING TIP — MODERATE BUFFET

**FIGURE 25. WINGLET FLOW IN LOW SPEED FLIGHT — INBOARD (SUCTION) SIDE,  
 $C_L = 1.5, V/V_{s_{MIN}} = 1.2$**

#### CONFIGURATION

- BASIC UPPER WINGLET WITH LOWER WINGLET
- NO LEADING EDGE DEVICE
- $\delta_F = 15 \text{ DEG}$
- $\delta_S = \text{TAKEOFF}$

UPPER WINGLET ATTACHED,  
LOWER WINGLET SEPARATED –  
MODERATE BUFFET

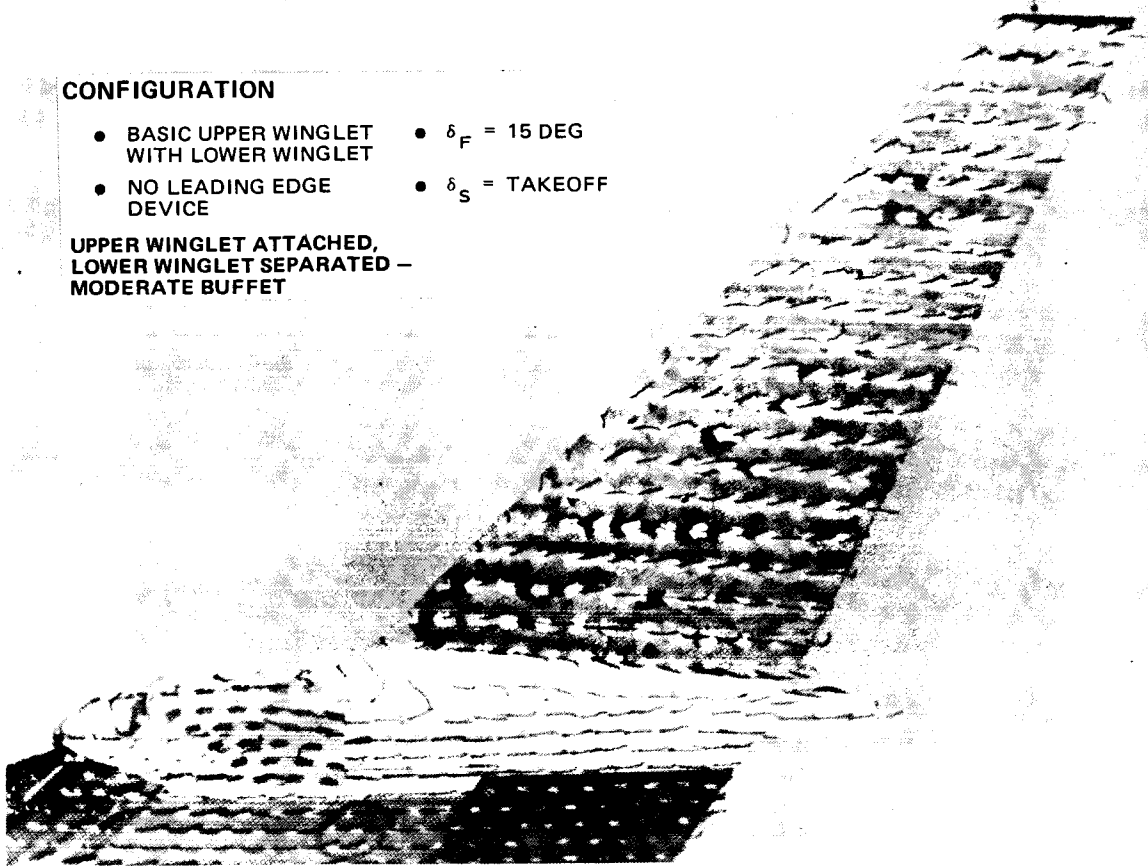


FIGURE 26. WINGLET FLOW IN LOW SPEED FLIGHT – OUTBOARD (PRESSURE) SIDE,  
 $C_L = 1.5, V/V_{S_{MIN}} = 1.2$

Figure 27 provides a summary of the configurations with the buffet and flow separation observed. The figure includes pilot's comments on the buffet levels for the speed condition corresponding to an all-engine takeoff ( $1.35 V_{MIN}$ ) and an engine-out takeoff ( $1.2 V_{MIN}$ ), and on the presence of the objectionable vertical bounce component in the buffet. The figure includes sketches of the flow visualization observed on the suction side of the upper and lower winglets, and peak-to-peak acceleration measured at the pilot's seat.

The consensus on the meaning of the acceleration measurements and their correlation with the flight experience was used to develop criteria for acceptability. The instrumentation system had an approximate 0.03g peak-to-peak noise level. Evaluation of the aircraft buffet characteristics without winglets indicated that they were in the normal range. The range of potentially acceptable configurations was determined to be from 0.03 to 0.06g depending on the buffet intensities caused by small changes in angle of attack and by normal maneuvering. The closer to 0.03, the higher the confidence level of acceptability. The presence of a vertical bounce component was deemed unacceptable.

The first attempt to eliminate the buffet problem was to install the Krueger flap (Configuration 2). The character of the flow was significantly different, but the buffet character remained

unchanged. Next, the lower winglet was removed because it was clear from the flow visualization that its separated flow wake was migrating into the root section of the upper winglet. With this configuration (Number 3), the buffet onset was improved, but the level of buffet at  $1.2 V_{MIN}$  was basically unchanged.

In order to relieve the root loading and to generate some vortex flow to help clean up the separation, a highly swept dorsal (Vortilet 1) was added to the unprotected root region (Configuration 4). The buffet levels as well as the amount of separated flow were reduced, but the configuration was still not acceptable.

Recognizing the importance of the root region, it was decided to remove the vortilet and extend the leading edge device down to the wing. This resulted in an acceptable configuration (Number 6). The flow was basically attached except for the small region at the tip which was not protected since the Krueger was not full span. The buffet intensity was significantly reduced, with the vertical bounce component barely perceptible. It was clear the the Krueger flap allowed the winglet to continue to load up as the airplane lift increased to the  $V_2$  condition.

Because of the importance of the lower winglet to cruise performance, it was reinstalled and the resulting configuration (Number 7) tested. Apparently the problem of the migration of the separated flow on the lower winglet into the upper winglet root region reoccurred because this configuration proved unacceptable.

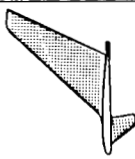
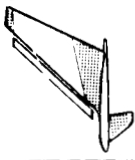
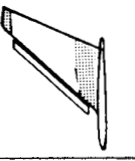
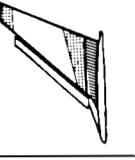
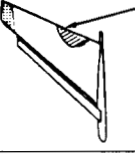
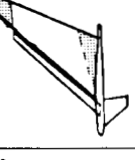
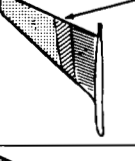
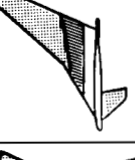
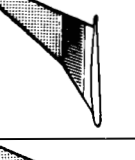
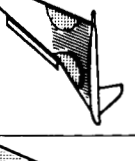
Both the Krueger flap and lower winglet were removed for cruise performance measurement (making Configuration 9), and during the flight the buffet characteristics were evaluated. The buffet was shown to be acceptable, but the flow on the winglet was still separated over 75 percent of the span. This separation was later shown to result in a significant reduction in the drag improvement due to the winglet.

In order to evaluate further the potential for an acceptable configuration without a leading edge device, an alternate planform (Vortilet 2) with modified airfoil leading edges (MOD 6) was evaluated. The airfoil modification was developed analytically, and the airfoil/planform change was evaluated in a concurrent Douglas low-Reynolds-number wind tunnel test on another transport configuration. The results indicated that the winglet remained separation-free down to the wing stall and thus represented potential for flight evaluation. However, none of the three versions (Configurations 10, 11, and 12 of Figure 20) of this planform proved acceptable in flight.

In summary, of all the basic winglet configurations evaluated for low-speed buffet characteristics, two (Configurations 6 and 9) were found to be acceptable.

$\delta_S = \text{TAKEOFF}$

$\delta_F = 15 \text{ DEGREES}$

CONFIGURATION NUMBER CONFIGURATION DESCRIPTION FLIGHT	1 BASIC UPPER AND LOWER WL A-17	2 UPPER AND LOWER WL WITH FCK AZ7	3 UPPER WL WITH FCK A-28	4 UPPER WL AND FCK AND VORTI A-29	6 UPPER WL AND FCK EXT A-31	7 UPPER AND LOWER WL AND FCK EXT AND FCK EXT A-32	9 UPPER WL ONLY A-44/A-45	10 VORT 2 WITH MOD 6 AND LOWER WL A-47	11 VORT 2 WITH MOD 6 W/O LOWER WL A-48	12 VORT 2 WITH FCK AND LOWER WL A-49
BUFFET AT 1.35 V <sub>MIN</sub>	LIGHT	LIGHT	VERY LIGHT	VERY LIGHT	NONE	PERCEPTIBLE	PERCEPTIBLE	LIGHT	LIGHT	LIGHT
BUFFET AT 1.20 V <sub>MIN</sub>	MODERATE	MODERATE	MODERATE	MODERATE	LIGHT	MODERATE	LIGHT	MODERATE	MODERATE	MODERATE
VERTICAL BOUNCE AT 1.20 V <sub>MIN</sub>	YES	YES	YES	YES	BARELY	YES	JUST BARELY	BARELY	BARELY	NO (LATERAL COMPONENT)
WING FLOW VISUALIZATION	SEPARATED	SEPARATED	SEPARATED	ATTACHED	ATTACHED	SEPARATED	ATTACHED	ATTACHED	ATTACHED	ATTACHED
WINGLET FLOW VISUALIZATION AT 1.20 V <sub>MIN</sub>										
PILOT SEAT ACCELERATION AT V = 1.20 V <sub>MIN</sub> (PEAK TO PEAK)	0.080	0.200	0.175	0.170	0.045	0.150	0.060	INSTRUMENTATION INOPERATIVE	INSTRUMENTATION INOPERATIVE	0.125

FLOW VISUALIZATION SHOWN ON THE INBOARD SURFACE OF UPPER WINGLET AND OUTBOARD SURFACE OF LOWER WINGLET



FIGURE 27. SUMMARY OF LOW-SPEED BUFFET CHARACTERISTICS - BASIC WINGLET

**Low-Speed Drag** – Figure 28 illustrates the flight-tested low-speed drag improvement for the basic winglet with extended Krueger leading edge flap on and lower winglet removed (Configuration 6). The data are relative to the baseline levels, and also are compared with wind tunnel results. At the lift coefficient representative of engine-out climb speed ( $V_2$ ), the winglet drag improvement is 5.7 percent for both flap deflections, equaling or exceeding pretest estimates based on wind tunnel data. It should be noted that the given wind tunnel data include the effect of the lower winglet. However, the wind tunnel investigation indicated a drag penalty for the leading edge device, whereas in flight the leading edge device effected a marked improvement in the flow separation characteristics of the upper winglet.

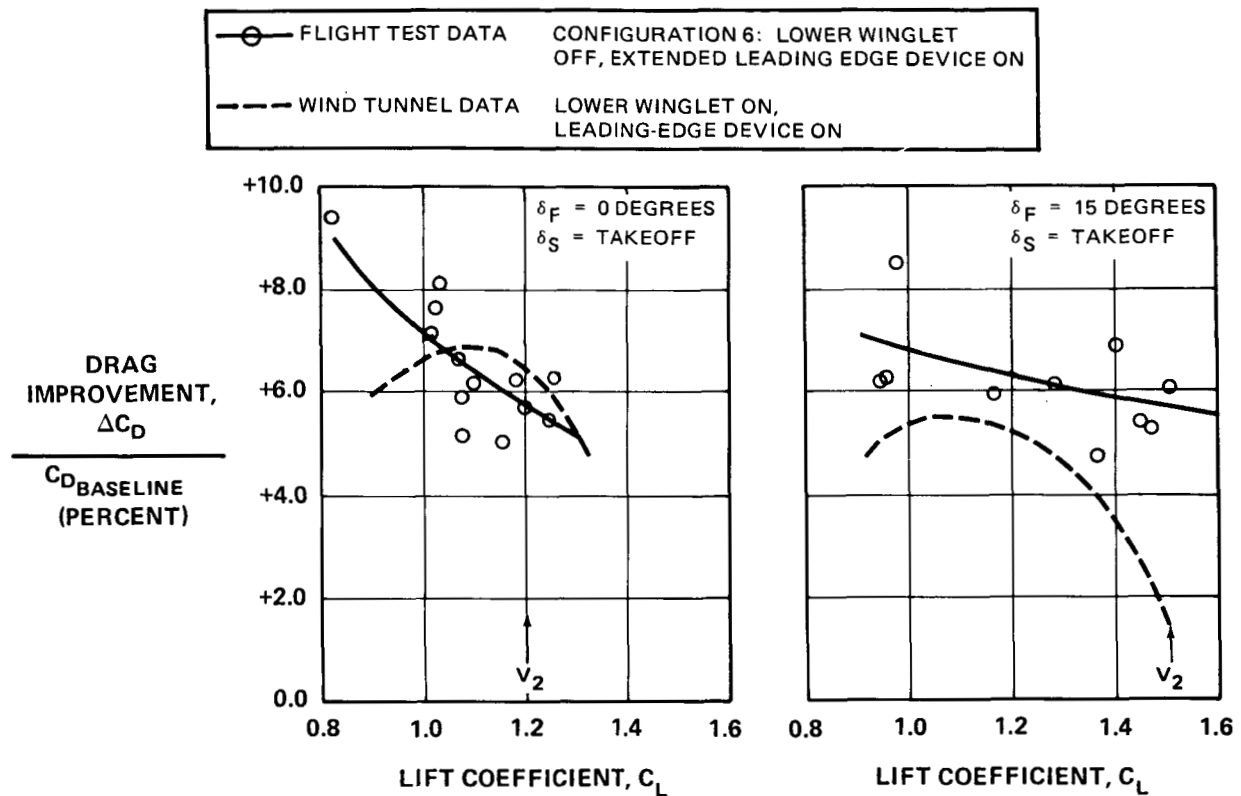


FIGURE 28. LOW SPEED DRAG IMPROVEMENT – BASIC WINGLET

**Stall Speeds and Characteristics** – Stall speeds were determined during both the baseline and winglet phases for three flap settings. It was evident that the aircraft stall speeds were essentially unaffected by the presence of winglets, as predicted by the wind tunnel results.

During the stall characteristics tests with winglets on, no unsatisfactory characteristics were recorded or reported by the flight crew.

**Cruise Performance** – The cruise performance improvement was determined from both the measured drag coefficient and range factor determinations. Excellent correlation was obtained

between these parameters, enabling the improvement to be described synonymously as a change in drag coefficient or range factor.

Figure 29 summarizes the cruise drag improvement for the basic winglet, given as the percent drag improvement relative to the baseline airplane. The improvement is shown with and without the lower winglet installed. Also shown is the wind tunnel prediction based on Reference 2 but adjusted for wing aeroelastic effects. With the lower winglet installed, the figure shows that the flight-measured level is about 0.4 percent less than the prediction at the highest lift coefficient of DC-10 Series 10 operation ( $C_L = 0.5$ ). At lower lift coefficients, the discrepancy was greater suggesting a significant parasite drag penalty at zero lift. At  $C_L = 0.47$ , a typical cruise number, the measured improvement is 2.5 percent compared to a predicted 3.4 percent (75 percent of prediction). The compressible and incompressible data are in good agreement.

It was evident, as shown in Figure 29, that the removal of the lower winglet resulted in a significant compressibility penalty, 1 percent at typical cruise  $C_L$ . The effect measured in the wind tunnel was 0.5 percent at compressible and incompressible Mach numbers.

Flow quality was examined through tuft photography at cruise conditions. The flow quality was excellent, with no indications of large spanwise flow areas or areas of flow separation.

In order to explain the apparent performance shortfall at the lower lift coefficients, the effects of winglets on wing bending and twist deflections were examined. Although flight test

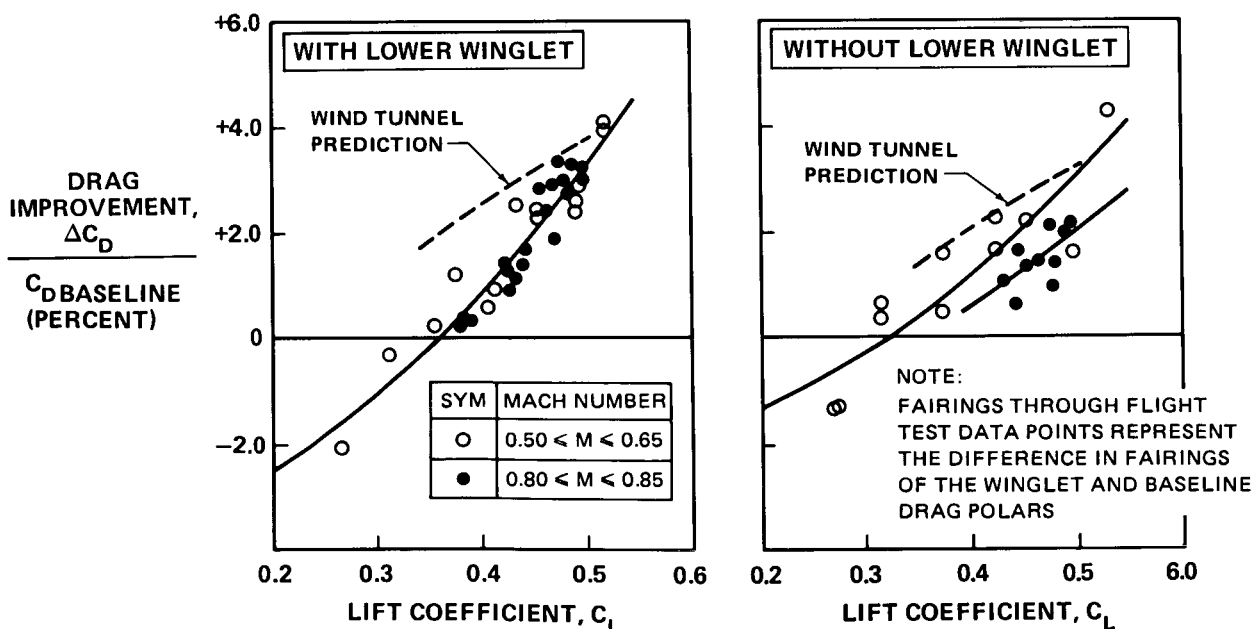


FIGURE 29. CRUISE DRAG IMPROVEMENT - BASIC WINGLET

measurements using the planned camera observation of wing surface targets proved to contain anomalies, deflection estimates were made using data from the loads measurement instrumentation. It was concluded that the derived wing deflections were in reasonable agreement with the preflight estimate included in the wind-tunnel curves of Figure 29.

Figure 30 shows the measured pressure distributions across the winglet span at 0.82 Mach number and 0.5 lift coefficient for Configuration 1. A significant leading edge suction peak is present resulting in a fairly strong shock wave, particularly on the winglet outer span. While the pressure distribution at the 12.5-percent station is in reasonably good agreement with the wind tunnel measurements, at the 80-percent station the shock appears to be significantly stronger both in peak Mach number and magnitude of compression. These stronger shocks may be adversely affecting cruise performance of the winglet. However, the lift coefficient reflected in the figure is the one where the measured benefit is closest to prediction (see Figure 29). Clearly, there may be compensating effects in the nature of the improvement characteristics, for example, shock losses being offset by the induced drag improvement due to the higher winglet loading.

The stronger shock wave on the outer panel was also evident at the lower lift coefficients. However, the strength did not appear stronger relative to the wind tunnel value than was measured at higher lift coefficients. These results suggest that at least part of the performance shortfall may be related to compressibility effects but that the trend with lift coefficients is not.

The upper winglet pressure distributions with the lower winglet off are compared in Figure 31 with those with the lower winglet. These pressures suggest that the additional penalty due to the removal of the lower winglet may be caused from shock losses on the inboard upper surface of the upper winglet. Outboard, the pressures are only slightly affected but inboard, the suction peaks are increased and the shock strengths have increased accordingly.

Winglet span loads and normal force coefficients showed excellent agreement with the wind tunnel-measured values, both in the level and the variation with airplane lift coefficient. In other words, the winglet was loading in flight in the way the wind tunnel data had predicted it would.

Excellent agreement was also found between flight and wind tunnel measurement of wingtip section loads.

**Cruise Buffet** — The results of the buffet tests are shown in Figure 32 as incremental buffet lift coefficients from the baseline airplane. The winglet results fall within the scatter band of the baseline aircraft and it is concluded that the winglet has little or no effect on the buffet boundary. In fact, for the 0.2g peak-to-peak level of normal acceleration (the value used for FAA certification), a slight improvement is indicated with the winglet, although there are insufficient data to substantiate this. These results agree with those of the wind tunnel tests.

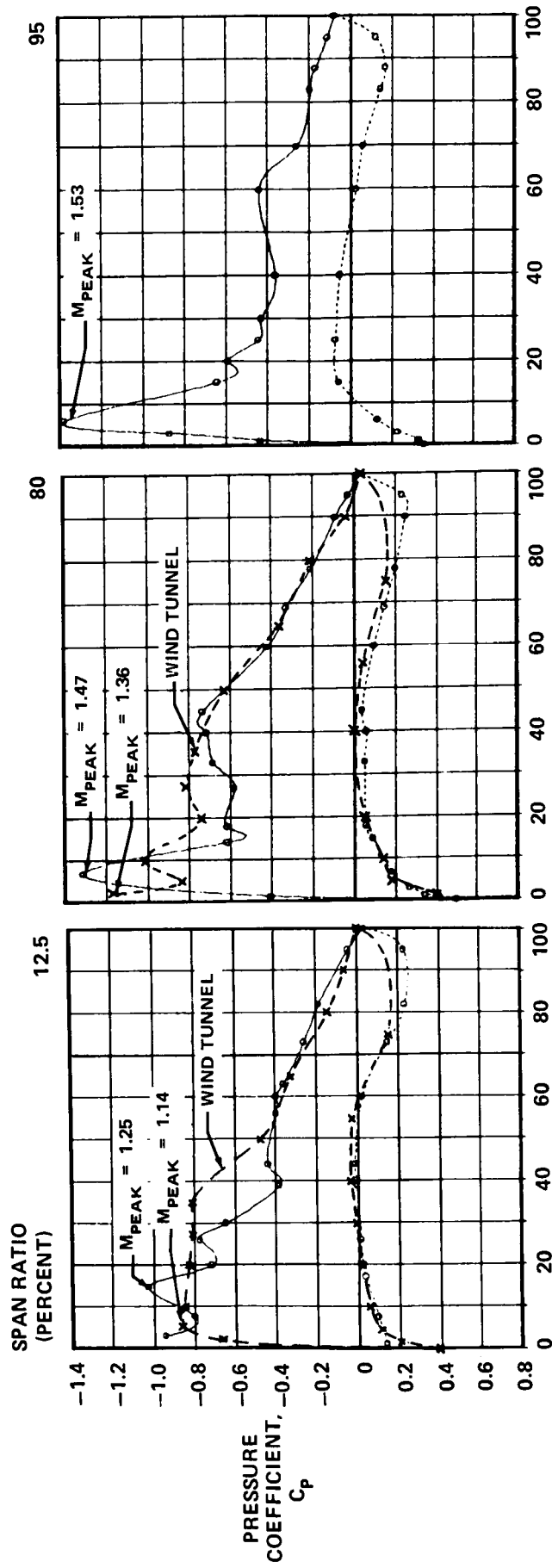


FIGURE 30. BASIC WINGLET PRESSURE DISTRIBUTION AT CRUISE

$M = 0.82, C_L = 0.5$

○ LOWER WINGLET ON  
△ LOWER WINGLET OFF

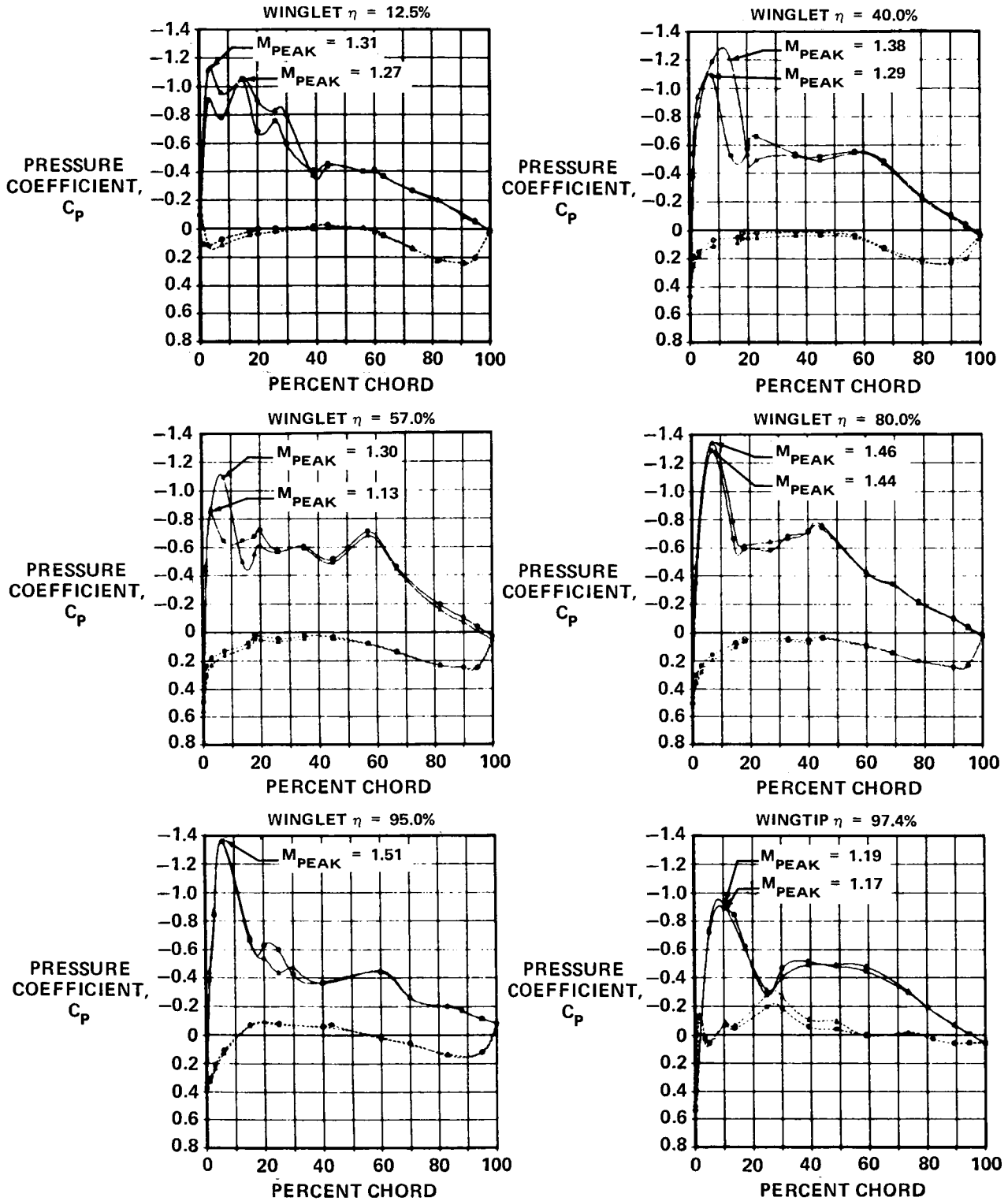


FIGURE 31. EFFECT OF LOWER WINGLET ON BASIC UPPER WINGLET/WINGTIP PRESSURE DISTRIBUTION AT CRUISE

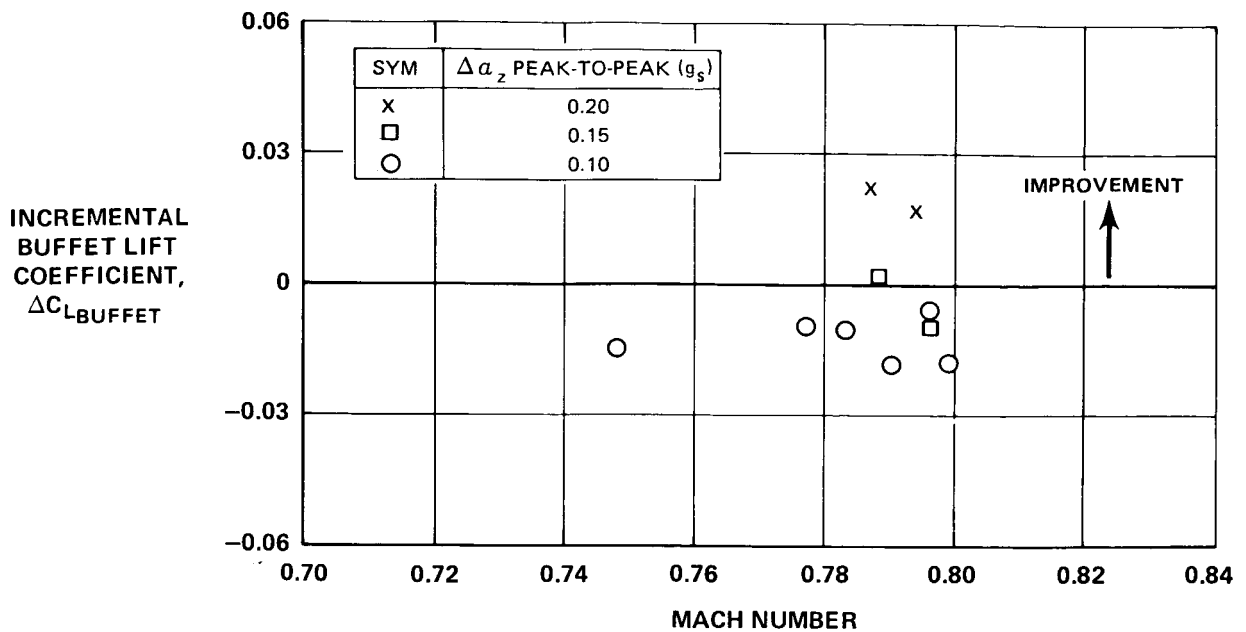


FIGURE 32. EFFECT OF BASIC WINGLET ON HIGH-SPEED BUFFET BOUNDARY

**Longitudinal Static Stability** — Increased longitudinal static stability due to winglets was predicted since the additional lift carried near the wing tip acts aft of the center of gravity and provides an airplane-nose-down moment. This result is shown by the test data in Figure 33 for a cruise and a climb condition compared with a calculation for the baseline aircraft.

**Longitudinal Maneuvering Stability** — The minimal effect of winglets on longitudinal maneuvering stability is shown by data from tests in the cruise and landing configurations (Figure 34). The small differences indicated between the baseline and winglet aircraft are considered to have been caused by instrumentation.

**Longitudinal Trim Characteristics** — In tests of the trim characteristics in cruise, the winglet data showed no significant change from the baseline trim levels. Correlation of the baseline flight test results and estimated values was very good.

**Static Directional Stability** — Tests were conducted for the baseline, BWL, and RSWL aircraft so that any variation in this sensitive parameter could be measured accurately. The data showed excellent correlation with calculated values and also showed that winglets have no noticeable effect on static directional stability.

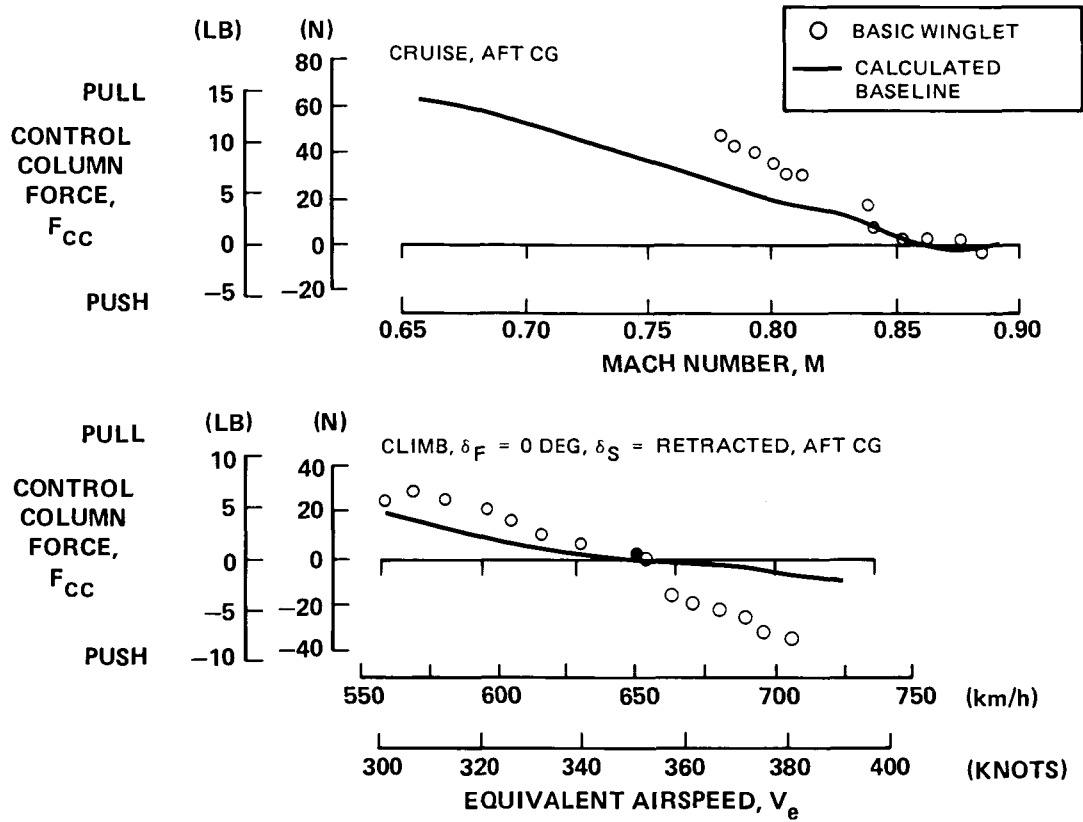


FIGURE 33. EFFECT OF BASIC WINGLET ON LONGITUDINAL STATIC STABILITY

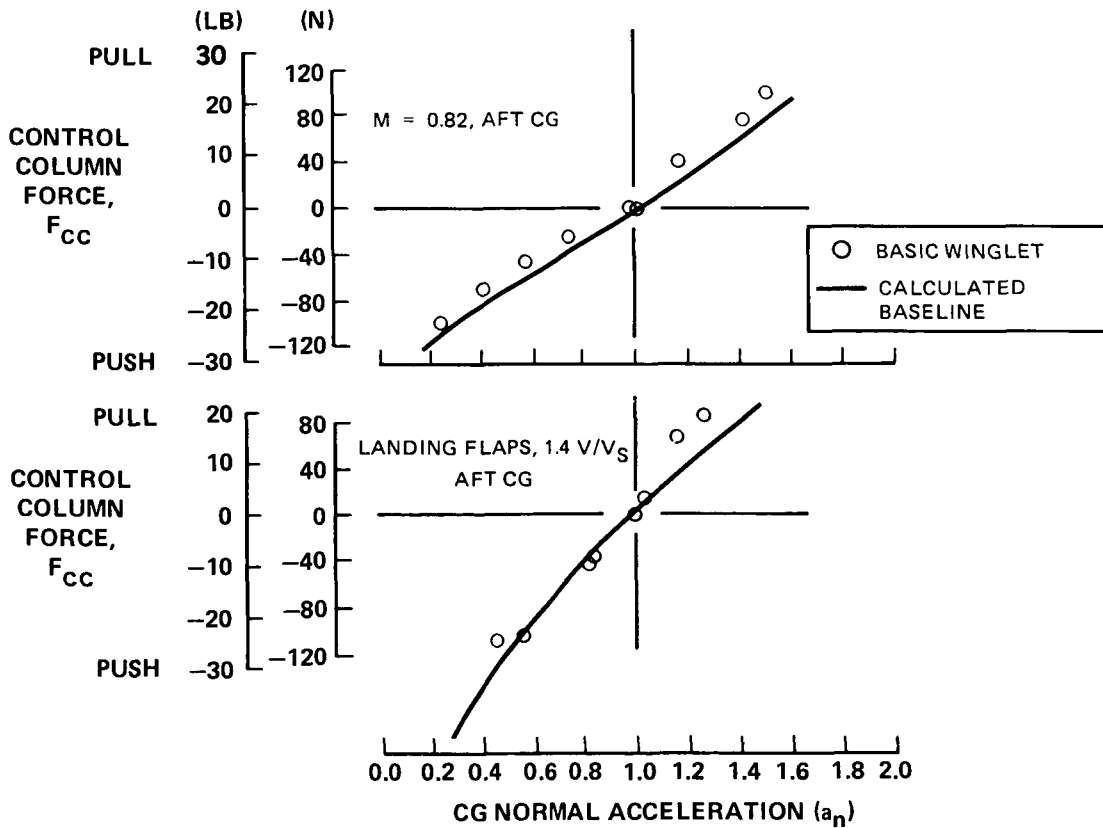


FIGURE 34. EFFECT OF BASIC WINGLET ON LONGITUDINAL MANEUVERING STABILITY

**Dynamic Lateral Stability (Dutch Roll)** — In the cruise configuration with the yaw dampers off, the time to damp to half amplitude was less than the calculated value for the baseline indicating that the Dutch-roll damping was greater than the baseline. In the landing configuration, the time to damp to half amplitude was greater than the baseline calculated values, indicating that the Dutch-roll damping was less than the calculated baseline.

**Spiral Stability and Roll Performance** — In each of these areas, it was concluded that the effect of winglets is very small.

**Loads Measurement** — The results indicate that:

- The measured winglet normal force levels were approximately at the expected levels.
- The variation of winglet normal force coefficient with aircraft angle of attack was in agreement with prediction.
- The effects of aeroelasticity were clearly evident.
- The measured increment of wing bending moment was generally as predicted. The horizontal bending effect resulting from the inboard acting winglet load and wing sweepback was also evident.
- Measured aileron loads were close to the predicted level.

### **Reduced-Span-Winglet Phase**

**Flight Test Program** — The planned objectives for the RSWL phase were met. Adjustments to the test details were made, considering effects of the insertion into the test program of the development activities and the good quality of the data in the BWL phase. Added to the program was an evaluation of the effect of drooping the outboard ailerons.

All the configurations tested during this phase are shown in Figure 35. As in the BWL phase, a leading edge device was tested at low speed. Configurations without such a device were tested both in the low-speed and high-speed regimes. The features of the configurations in the figure, which are also illustrated by the photographs of Figure 36, are as follows:

- Configuration 13: Upper Krueger flap extended root to tip, no lower winglet. The extent of this flap is shown in Figure 36, together with features of the later Configuration 17.
- Configuration 14: Upper winglet only.
- Configuration 15: Configuration 14 with lower winglet.

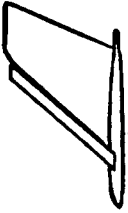
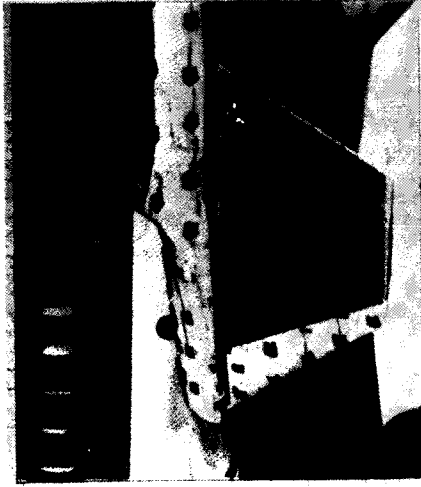
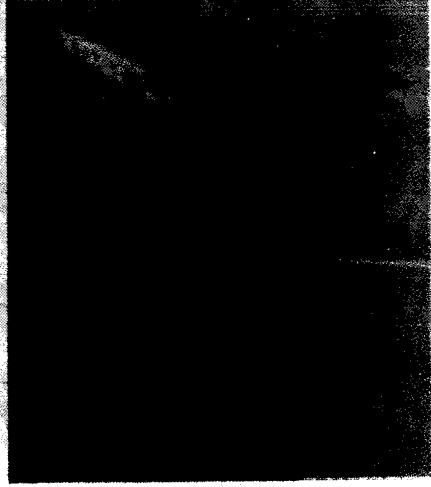
CONFIGURATION NUMBER	PHYSICAL APPEARANCE	DESCRIPTION	FLIGHTS WHICH EMPLOYED CONFIGURATION
13		REDUCED-SPAN WINGLET WITH KRUEGER FLAP INSTALLED WITH EXTENSION TO WING TIP. KRUEGER FLAP DEFLECTION WAS 40 DEGREES	A50
14		REDUCED-SPAN UPPER WINGLET WITHOUT LOWER WINGLET	A51-A53
15		REDUCED-SPAN UPPER WINGLET WITH BASIC LOWER WINGLET INSTALLED	A54-A56
16		CONFIGURATION NUMBER 13 WITH BASIC LOWER WINGLET INSTALLED	A57
17		CONFIGURATION NUMBER 13 WITH 80-PERCENT EXTENDED CHORD LOWER WINGLET INSTALLED. LOWER WINGLET HAD SEALED KRUEGER FLAP INSTALLED	A58
18		REDUCED-SPAN UPPER WINGLET WITH 80-PERCENT EXTENDED CHORD LOWER WINGLET INSTALLED. (NO LEADING EDGE DEVICES ON UPPER OR LOWER WINGLET)	A59-A60
19		CONFIGURATION NUMBER 18 WITH OUTBOARD AILERONS DROOPED 3.0 DEGREES	A61

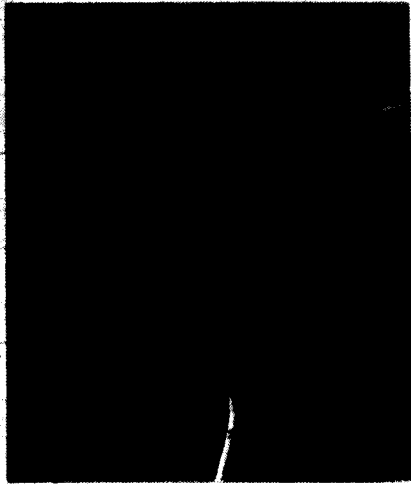
FIGURE 35. CONFIGURATION IDENTIFICATION FOR REDUCED-SPAN WINGLET FLIGHT PROGRAM



7-FOOT UPPER WINGLET AND  
80-PERCENT EXTENDED CHORD  
LOWER WINGLET



LOWER WINGLET KRUEGER FLAP



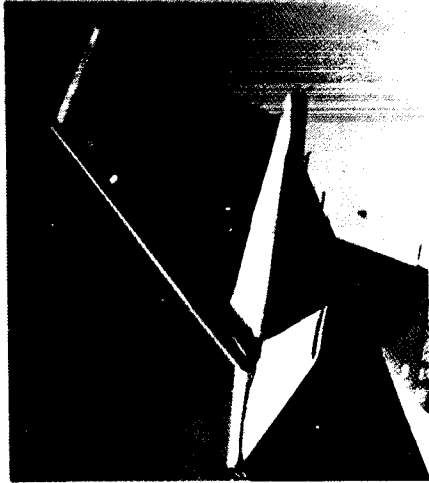
7-FOOT UPPER WINGLET WITHOUT  
LOWER WINGLET



LOWER WINGLET KRUEGER FLAP



7-FOOT UPPER WINGLET  
AND 2.5-FOOT LOWER WINGLET



UPPER WINGLET KRUEGER FLAP

FIGURE 36. REDUCED-SPAN WINGLET CONFIGURATIONS

- Configuration 16: Configuration 13 with lower winglet.
- Configuration 17: Configuration 13 with modified (extended chord) lower winglet. This winglet had a chord extension of 80 percent of the local chord of the basic original lower winglet. The extension was made aft from the leading edge. The leading edge shape forward of the front spar was retained.
- Configuration 18: Configuration 17 without leading edge devices.
- Configuration 19: Configuration 18 with outboard ailerons drooped 3 degrees (measured in the streamwise direction) from the basic rigged position.

In the BWL phase discussion, it was noted that the evolution of a satisfactory winglet should balance or resolve the apparently opposing requirements for and against the lower winglet. On the one hand, the lower winglet improved cruise performance; on the other, it contributed adversely to the low-speed buffet. An attempt to resolve this opposition led to the extended-chord lower winglet, whose design was aided by NASA Langley investigators. It was reasoned that such a chord extension would reduce the local section lift coefficients on the lower winglet and thus delay flow separation on the lower winglet to a higher level of aircraft lift coefficient. However, there was concern over the potential degradation of cruise performance since during the wind tunnel tests overlap of the lower and upper winglets was identified as a potential problem area. Therefore, a number of tests were made with this configuration in various forms.

**Low-Speed Buffet** — Figure 37 summarizes the low-speed buffet results. Configuration 13, the first tested, was directly related to the most promising BWL configuration. Like the most promising BWL, this configuration exhibited acceptable buffet characteristics.

Since removing the Krueger flap on the BWL resulted in acceptable buffet characteristics even though there was extensive flow separation, a similar configuration (Number 14) was tested next. Acceptable buffet characteristics were achieved, but again the flow on the winglet was about 75-percent separated, which would adversely affect the drag improvement.

During the cruise-data-gathering flight for the configuration with the upper and lower winglets installed (Configuration 15), the low-speed buffet was also evaluated and was found to be acceptable. It was clear that the lower aspect ratio of the reduced-span winglet or its structural response to the separated flow was having a significantly favorable effect on buffet characteristics.

Structural response was measured during flight, the data being used to generate power spectral densities (PSDs) showing vibratory power as a function of buffet frequency. Figure 38 presents a comparison of buffet response data for the BWL and RSWL configurations. The data show that the PSD levels with the RSWL are significantly lower than those with the BWL, and

$\delta_F = 15$  DEGREES  $\delta_S =$  TAKEOFF

CONFIGURATION NUMBER	CONFIGURATION DESCRIPTION	13	14	15	16	17	18	19
	FLIGHT	UPPER WL AND FCK EXT A-50	UPPER WL A-52	UPPER WL WITH LOWER WL A-54	UPPER WL WITH FCK EXT AND LOWER WL A-57	UPPER WL WITH FCK EXT AND LOWER EXT WL WITH FCK A-58	UPPER WL AND LOWER EXT WL A-59	UPPER WL AND LOWER EXT WL AND DROOPED AILERON A-61
	BUFFET AT 1.35 V <sub>MIN</sub>	NONE	NONE	PERCEPTIBLE	LIGHT	NONE	VERY LIGHT	PERCEPTIBLE
	BUFFET AT 1.20 V <sub>MIN</sub>	PERCEPTIBLE	LIGHT	LIGHT	MODERATE	BARELY PERCEPTIBLE	LIGHT	LIGHT
	VERTICAL BOUNCE AT 1.20 V <sub>MIN</sub>	NO	NO	NO	NO	NO	NO	NO
	WING FLOW VISUALIZATION	ATTACHED	ATTACHED	NO FLOW VISUALIZATION	ATTACHED	ATTACHED	SEPARATED	NO FLOW VISUALIZATION
	WINGLET FLOW VISUALIZATION AT 1.20 V <sub>MIN</sub>	ATTACHED	ATTACHED	NO FLOW VISUALIZATION	ATTACHED	ATTACHED	SEPARATED	NO FLOW VISUALIZATION
	PILOT SEAT ACCELERATION AT V = 1.20 V <sub>MIN</sub> (PEAK-TO-PEAK)	0.03	0.04	0.04	0.07	0.04	0.05	0.06



FLOW VISUALIZATION SHOWN ON THE INBOARD SURFACE OF UPPER WINGLET AND OUTBOARD SURFACE OF LOWER WINGLET

FIGURE 37. SUMMARY OF LOW-SPEED BUFFET CHARACTERISTICS - REDUCED-SPAN WINGLET

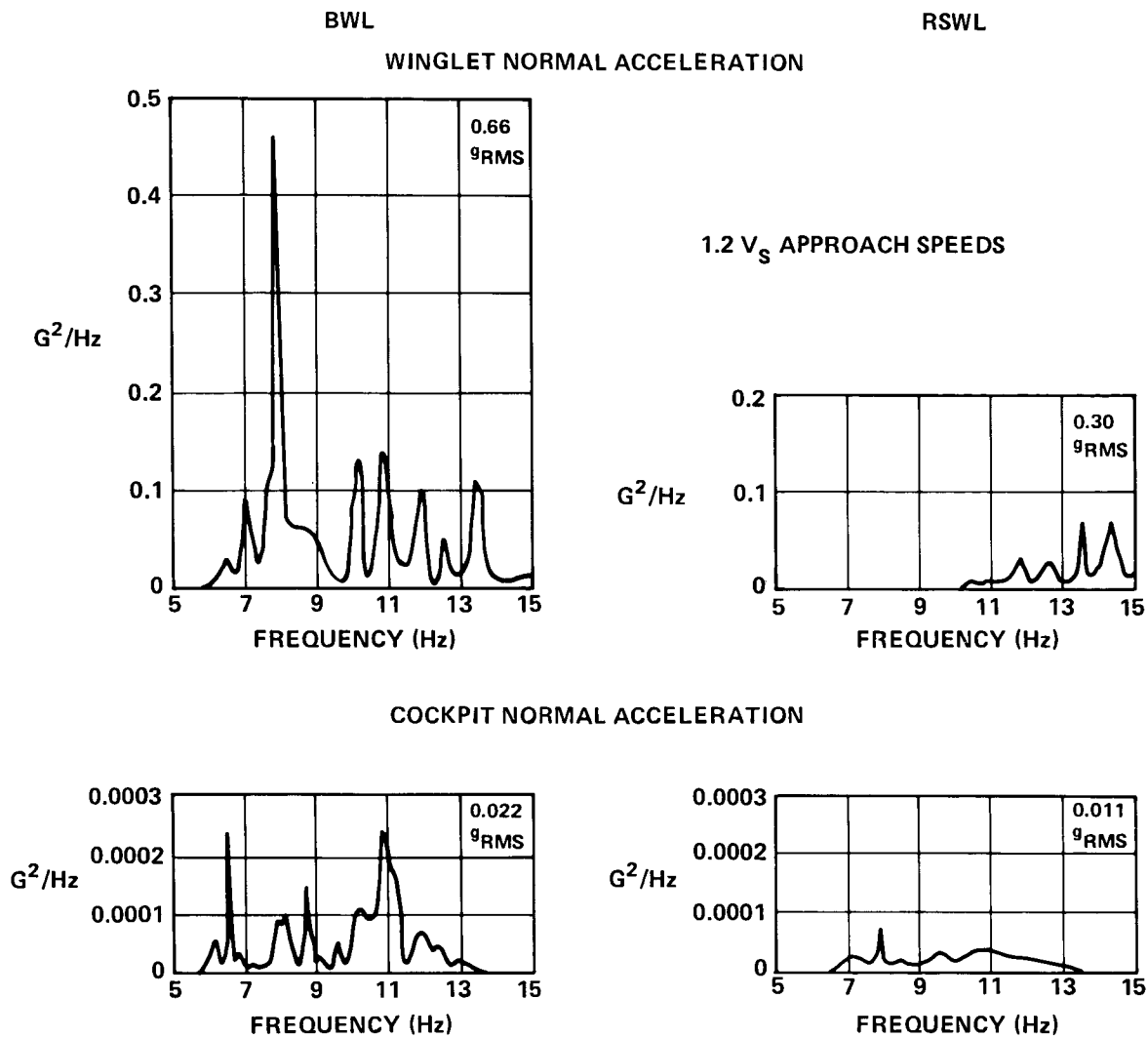


FIGURE 38. BUFFET RESPONSE ACCELERATION POWER SPECTRA

that root mean square values are approximately half. The data indicate that the cockpit response is the result of several structural modes being excited, most probably by the aerodynamic forcing function due to flow separation. However, no correlation appears obvious between the shape of the acceleration power spectrum and the size of the winglet or the degree of separation.

The remaining configurations evaluated (Numbers 15 through 19) were aimed at finding the best overall configuration from the standpoints of buffet, low-speed drag improvement, and cruise drag improvement. All except Configuration 16 were acceptable from a buffet standpoint.

Configuration 17, which employed the extended chord lower winglet with a leading edge device, did not prevent flow separation on the lower winglet at V<sub>2</sub> conditions. However, the flow on the leading edge device itself stayed attached, thus providing significant leading edge suction. In addition, the wake from the separated flow did not go over the wing.

**Low-Speed Drag** — Figure 39 shows the low-speed drag improvement for Configuration 13 (extended upper leading edge devices, no lower winglet), Configuration 14 (Configuration 13 with no leading edge devices), and Configuration 17 (Configuration 13 with extended chord lower winglet and leading edge devices on both winglets). The figure shows a drag improvement of approximately 80 percent of the BWL, both having leading edge devices. Removal of the upper winglet leading edge device resulted in more than a 50-percent loss in performance improvement (from 4.4 percent to 2.1 percent) at  $V_2$  conditions. This loss was caused by the flow separation on the inboard surface of the upper winglet. The lower winglet had a favorable impact showing an additional 1.5-percent improvement at  $V_2$  conditions. The resulting low-speed drag improvement at  $V_2$  for the RSWL with the lower winglet was 5.9 percent, exceeding the value obtained for the BWL without the lower winglet. It can be inferred that the BWL configuration with a lower winglet equipped with a leading edge device would probably have provided acceptable buffet characteristics and a performance improvement similar to that measured on the RSWL.

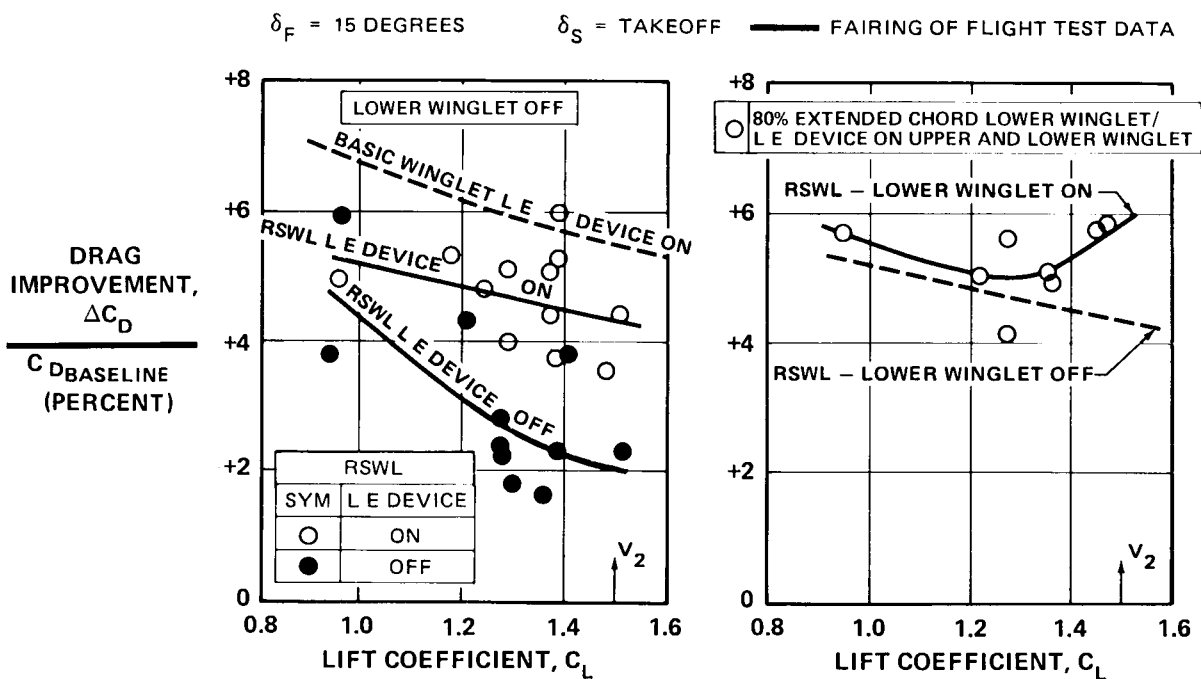


FIGURE 39. LOW SPEED DRAG IMPROVEMENT — REDUCED-SPAN WINGLET

**Cruise Performance** — The cruise drag benefit is shown in Figure 40. With the lower winglet installed (Configuration 15) and at the typical cruise  $C_L$ , the improvement is about 2 percent. This is only 0.5 percent less than the BWL while the predicted difference was 1 percent. The slope of the flight-measured improvement with lift coefficient is closer to the prediction than it was for the BWL. The figure also shows the detrimental compressible effect due to removal of the lower winglet to be of similar magnitude to that of the BWL.

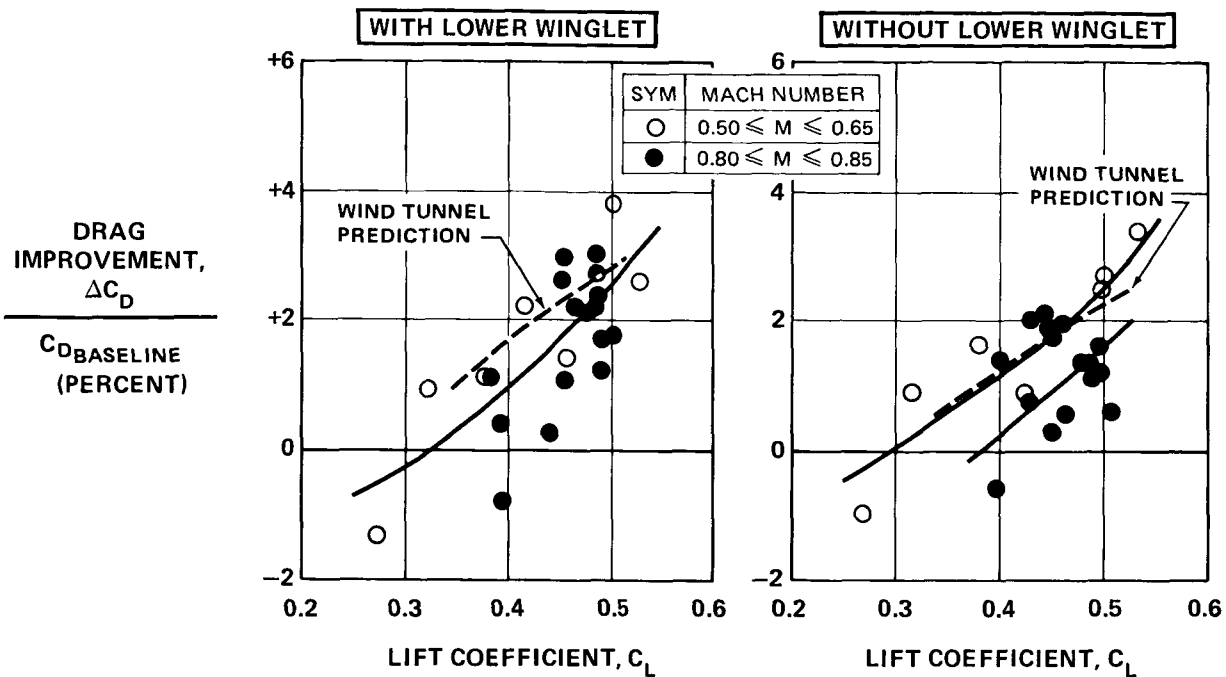


FIGURE 40. CRUISE DRAG IMPROVEMENT – REDUCED-SPAN WINGLET

Test data showed that the span reduction effectively eliminated the very high suction peaks that occurred on the outer span of the BWL. The data also showed that removal of the lower winglet resulted in increased upper winglet loading and increased suction peaks, similar in nature to the BWL. It can be inferred from the pressure data that the high suction peaks on the outer span of the BWL contributed to its performance shortfall, and that an improvement probably could be effected by redesign.

The two major configuration changes made during this phase were the extended-chord lower winglet (Configuration 18) and the use of drooped outboard ailerons (Configuration 19). Figure 41 shows the results of their cruise performance evaluation, shown as a deviation from the respective comparison configurations. Compared with Configuration 16, a slight penalty is indicated for the extended-chord winglet. There was no evidence of flow separation on the lower winglet. Compared with Configuration 18, drooping the ailerons showed an improvement of 1 percent, which agreed with the analytical estimate for this design. Pressure data showed that both the winglet and the wing tip were loaded more with the aileron droop. The benefit arises from these increases in loading.

Configuration 19 was the best for improving cruise drag. At  $C_L = 0.47$ , the measured drag improvement was 2.8 percent. If the extended-chord lower winglet, which showed a small penalty by itself, was replaced with the original lower winglet, a configuration with a nominal cruise drag improvement of about 3 percent would be expected.

SYMBOL	MACH NUMBER
○	0.50 < M < 0.65
●	0.80 < M < 0.85

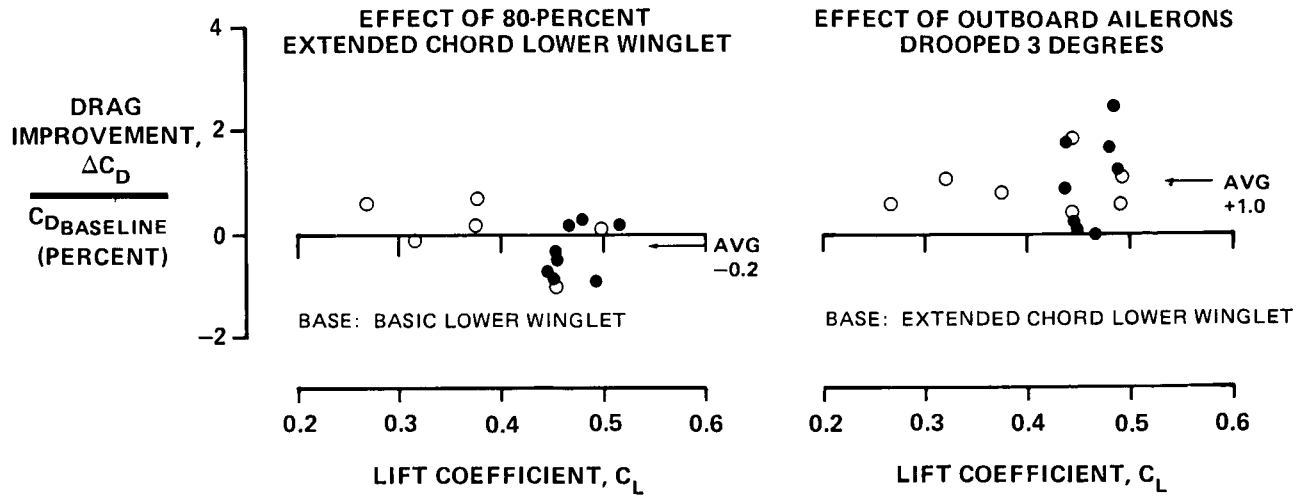


FIGURE 41. EFFECT OF CONFIGURATION VARIABLES ON CRUISE DRAG IMPROVEMENT - REDUCED-SPAN WINGLET

## IMPACT OF FLIGHT EVALUATION RESULTS ON OPERATIONAL PERFORMANCE

The data obtained during the flight evaluation were used to estimate the configuration and performance effects of winglets on a derivative version of a DC-10 Series 10 transport. The Series 10 used in this evaluation carries 297 passengers and a maximum payload of 26 943 kg (53,000 lb) including full passenger and baggage load. Its maximum takeoff gross weight is 195 045 kg (430,000 lb) and it is powered by three General Electric CF6-6D engines rated at 177,9 kN (40,000 lb) sea level static thrust.

The winglet configurations used were the BWL, the RSWL, and the RSWL with aileron droop. Each had upper and lower winglets with winglet leading-edge devices deployed for takeoff and landing. The original basic planform without chord extensions was used for the lower winglet.

The flight-measured loads were used to determine the increase in operator empty weight ( $\Delta$ OEW) for the production installation of the winglets, shown in Figure 42.

The impact of the three winglet configurations on key operating conditions is summarized in Figure 43. At a range of 3 704 km (2,000 n mi), representative of typical Series 10 operation, the best winglet configuration results in a 2.7-percent fuel-burn improvement (this increases to 3 percent at maximum range). At the maximum takeoff gross weight the range is increased 113 km (61 n mi) and the field length is reduced 162 m (530 ft).

	$\Delta$ OEW $\approx$ kg (LB)					
	BASIC WINGLET		REDUCED-SPAN WINGLET		REDUCED-SPAN WINGLET WITH AILERON DROOP	
WINGLET	382	(842)	321	(708)	321	(708)
WING						
BOX (BENDING)	207	(457)	83	(183)	135	(298)
BOX (SHEAR)	10	(22)	1	(2)	2	(4)
SLATS, FLAPS, AILERON	72	(159)	58	(128)	92	(203)
FLUTTER	635	(1,400)	136	(300)	136	(300)
SYSTEMS	34	(75)	34	(75)	59	(130)
TOTAL	1,340	(2,955)	633	(1,396)	745	(1,643)

**FIGURE 42. INCREASES IN OPERATOR'S EMPTY WEIGHT**

DRAG AND WEIGHT CHANGES	BASIC WINGLET	REDUCED-SPAN WINGLET	REDUCED-SPAN WINGLET PLUS AILERON DROOP
CRUISE DRAG IMPROVEMENT = PERCENT	2.5	2.0	3.0
OPERATOR EMPTY WEIGHT = kg (LB)	1,340 (2,955)	633 (1,396)	745 (1,643)
LOW SPEED DRAG IMPROVEMENT = PERCENT	6.8	5.8	5.8
AIRCRAFT PERFORMANCE CHANGES			
FUEL BURNED = PERCENT			
AT 3,704 km (2,000 N MI)	-1.8	-1.7	-2.7
AT 6,112 km (3,300 N MI)	-2.1	-2.0	-3.0
RANGE = km (N MI)	-9 (-5)	+59 (+32)	+113 (+61)
TAKEOFF FIELD LENGTH = m (FT) AT MTOGW	-198 (-650)	-162 (-530)	-162 (-530)

FIGURE 43. EFFECT OF WINGLETS ON DC-10 SERIES 10 PERFORMANCE CHARACTERISTICS

Fuel-burn improvement versus range is shown in Figure 44. The basic and reduced-span winglets show about the same improvement, nearly 2 percent. While the basic winglet drag improvement is higher than that for the reduced-span winglet, the higher  $\Delta$ OEW almost negates the added drag benefit. For only a small weight penalty, the drooped ailerons provided an additional 1-percent reduction in fuel burned.

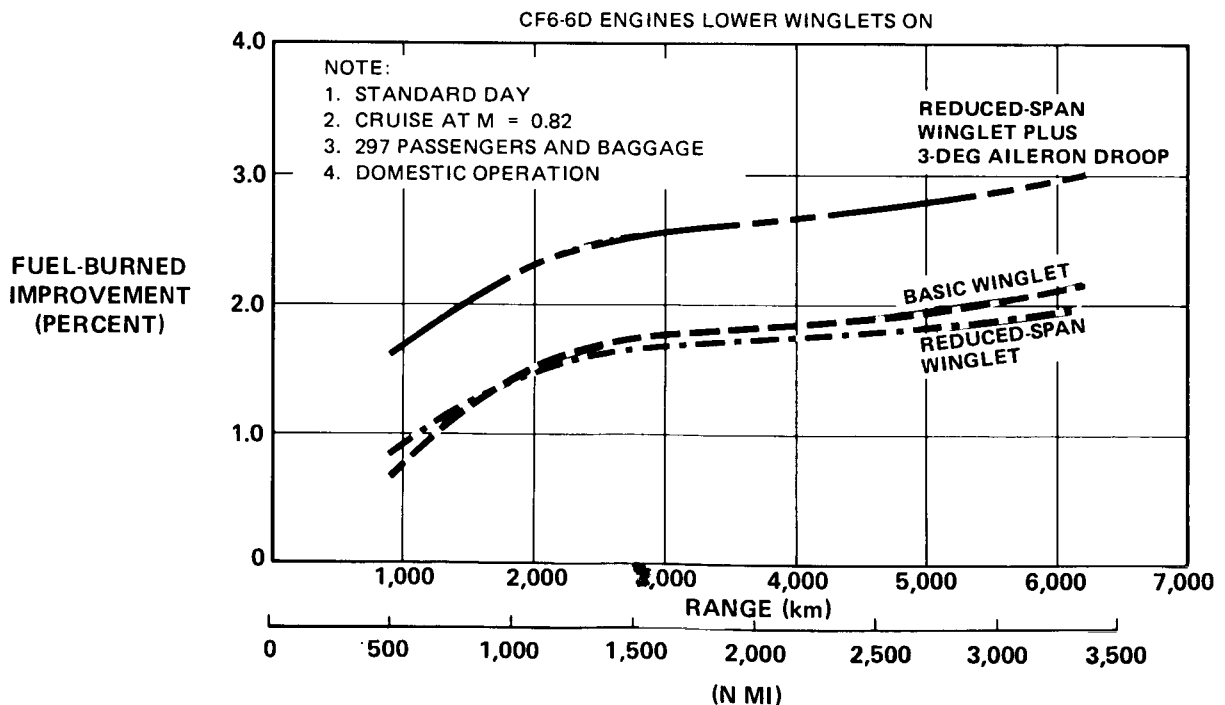


FIGURE 44. EFFECT OF WINGLET CONFIGURATIONS ON FUEL BURNED

## CONCLUSIONS

As a result of the DC-10 winglet flight evaluation, it was determined that:

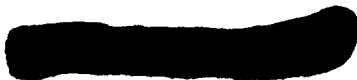
1. The drag reduction at typical cruise operating conditions for the basic winglet was 2.5 percent and for the reduced-span winglet, 2.0 percent. This was about 75 percent of the level predicted using wind tunnel test data.
2. Removal of the lower winglet significantly detracted from the cruise performance benefit, reducing it by about 1 percent.
3. Drooping the outboard ailerons 3 degrees resulted in an additional cruise drag reduction of 1 percent (only tested on the reduced-span winglet.)
4. Flow separation was experienced on the winglets in the low-speed/high-lift configuration resulting in aircraft buffet for some configurations. A winglet leading edge device eliminated the flow separation.
5. For the basic winglet configurations evaluated, acceptable low-speed buffet/performance characteristics were achieved with a leading edge device on the upper winglet and the lower winglet removed. The low-speed drag reduction for this configuration exceeded 5 percent, which was better than expected.
6. For the reduced-span winglet, acceptable low-speed buffet characteristics were achieved with or without either the winglet leading edge devices or the lower winglet. The low-speed drag improvement was nearly 6 percent with the leading edge devices installed.
7. Removal of the leading edge devices and the lower winglet reduced the low-speed drag improvement to 2 percent.
8. Stability and control characteristics, minimum stall speeds, and the high-speed buffet boundary were basically unchanged by the winglets.
9. The loads measurements were in good agreement with preflight estimates.
10. The flutter test did not reveal any unforeseen behavior, and the data showed good agreement with ground vibration test and analysis data.

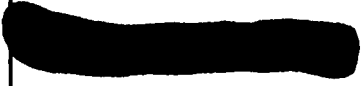
11. Application of the reduced-span winglet with aileron droop to a production DC-10 Series 10 is estimated to yield the following at maximum range:

- 3-percent reduction in fuel burned
- 113-km (61-n-mi) increase in range
- 162-m (530-ft) reduction in takeoff field length.

## REFERENCES

1. Whitcomb, R. T., A Design Approach and Selected Wind-Tunnel Results at High Subsonic Speeds for Wing-Tip Mounted Winglets. NASA TN D-8260, July 1976.
2. Gilkey, R. D., Design and Wind Tunnel Tests of Winglets on a DC-10 Wing. NASA CR-3119, April 1979.
3. Shollenberger, C.A., Humphreys, J. W., Heiberger, F. S., and Pearson, R. M., Results of Winglet Development Studies for DC-10 Derivatives. NASA CR-3677, March 1983.
4. Staff of Douglas Aircraft Company, DC-10 Winglet Flight Evaluation. NASA CR-3704, June 1983.



1. Report No. NASA CR-3748		2. Government Accession No.		3. Recipient's Catalog No.	
4. Title and Subtitle DC-10 WINGLET FLIGHT EVALUATION SUMMARY REPORT				5. Report Date December 1983	
				6. Performing Organization Code	
7. Author(s) A. B. Taylor				8. Performing Organization Report No. ACEE-17-FR-2836A	
9. Performing Organization Name and Address Douglas Aircraft Company McDonnell Douglas Corporation 3855 Lakewood Boulevard Long Beach, CA 90846				10. Work Unit No.	
				11. Contract or Grant No. NAS1-15327 (TASK 7)	
12. Sponsoring Agency Name and Address National Aeronautics and Space Administration Washington, DC 20546				13. Type of Report and Period Covered Contractor Report August 1980 - April 1982	
				14. Sponsoring Agency Code	
15. Supplementary Notes Langley Technical Monitor: Thomas G. Gainer Summary Report under TASK 7					
16. Abstract <p>The report summarizes the results of a flight evaluation of winglets on a DC-10 Series 10 aircraft. For sensitive areas of comparison, effects of winglets were determined back-to-back with and without winglets. Basic and reduced-span winglet configurations were tested.</p> <p>After initial encounter with low-speed buffet, a number of acceptable configurations were developed. For maximum drag reduction at both cruise and low speeds, lower winglets were required, having leading edge devices on upper and lower winglets for the latter regime. The cruise benefits were enhanced by adding outboard aileron droop to the reduced-span winglet aircraft. Winglets had no significant impact on stall speeds, high-speed-buffet boundary, and stability and control characteristics. Flutter test results agreed with predictions and ground vibration data. Flight loads measurement, provided in a concurrent Douglas program, also agreed with predictions.</p> <p>It was estimated from the results that a production version of the aircraft, using the reduced-span winglet and aileron droop, would yield a 3-percent reduction in fuel burned at the range with capacity payload. This range was 2 percent greater than without winglets. A 5-percent reduction in takeoff distance at maximum takeoff weight would also result.</p>					
17. Key Words (Suggested by Author(s)) Winglets Energy Efficient Transport Project Drag Reduction, Stability and Control, and Flutter Aircraft			18. Distribution Statement  Subject Category 05		
19. Security Classif. (of this report) Unclassified		20. Security Classif. (of this page) Unclassified		21. No. of Pages 68	22. Price